Chapter 1. Interagency Monitoring of Protected Visual Environments (IMPROVE) Network: Configuration and Measurements

1.1 INTRODUCTION

The Regional Haze Rule (RHR, U.S. EPA, 1999a) requires monitoring in locations representative of the 156 visibility-protected federal Class I areas (CIA, see Figure 1.1) in order to track progress toward the goal of returning visibility to natural conditions. Air quality monitoring under the RHR began in 2000. The haziness index in deciview units (Pitchford and Malm, 1994), calculated from speciated particle composition concentrations, was selected to track haze levels for the RHR. Computing the haziness index from particle speciation data entails sampling and analysis of major aerosol species, using methods employed by the IMPROVE network since 1987 (Joseph et al., 1987; Malm et al., 1994; Sisler, 1996). These methods are consistent with the aerosol monitoring portion of the 1999 Visibility Monitoring Guidance document issued by the U.S. Environmental Protection Agency (EPA) (U.S. EPA, 1999b).

The IMPROVE program is a cooperative measurement effort designed to

1. establish current visibility and aerosol conditions in mandatory CIAs;
2. identify chemical species and emission sources responsible for existing anthropogenic and natural visibility impairment;
3. document long-term trends for assessing progress towards the national visibility goal;
4. and, with the enactment of the RHR, provide regional haze monitoring representing all visibility-protected federal CIAs where practical.

The program is managed by the IMPROVE steering committee, which consists of representatives from the EPA; the four federal land managers (FLMs): the National Park Service, U.S. Forest Service, U.S. Fish and Wildlife Service, and Bureau of Land Management; the National Oceanic and Atmospheric Administration; four organizations representing state air quality organizations: the State and Territorial Air Pollution Program Administrators/Association of Local Air Pollution Control Officials (STAPA/ALAPCO), Western Regional Air Partnership (WRAP), Northeast States for Coordinated Air Use Management (NESCAUM), and Mid-Atlantic Regional Air Management Association (MARAMA); and an associate member, the State of Arizona Department of Environmental Quality.

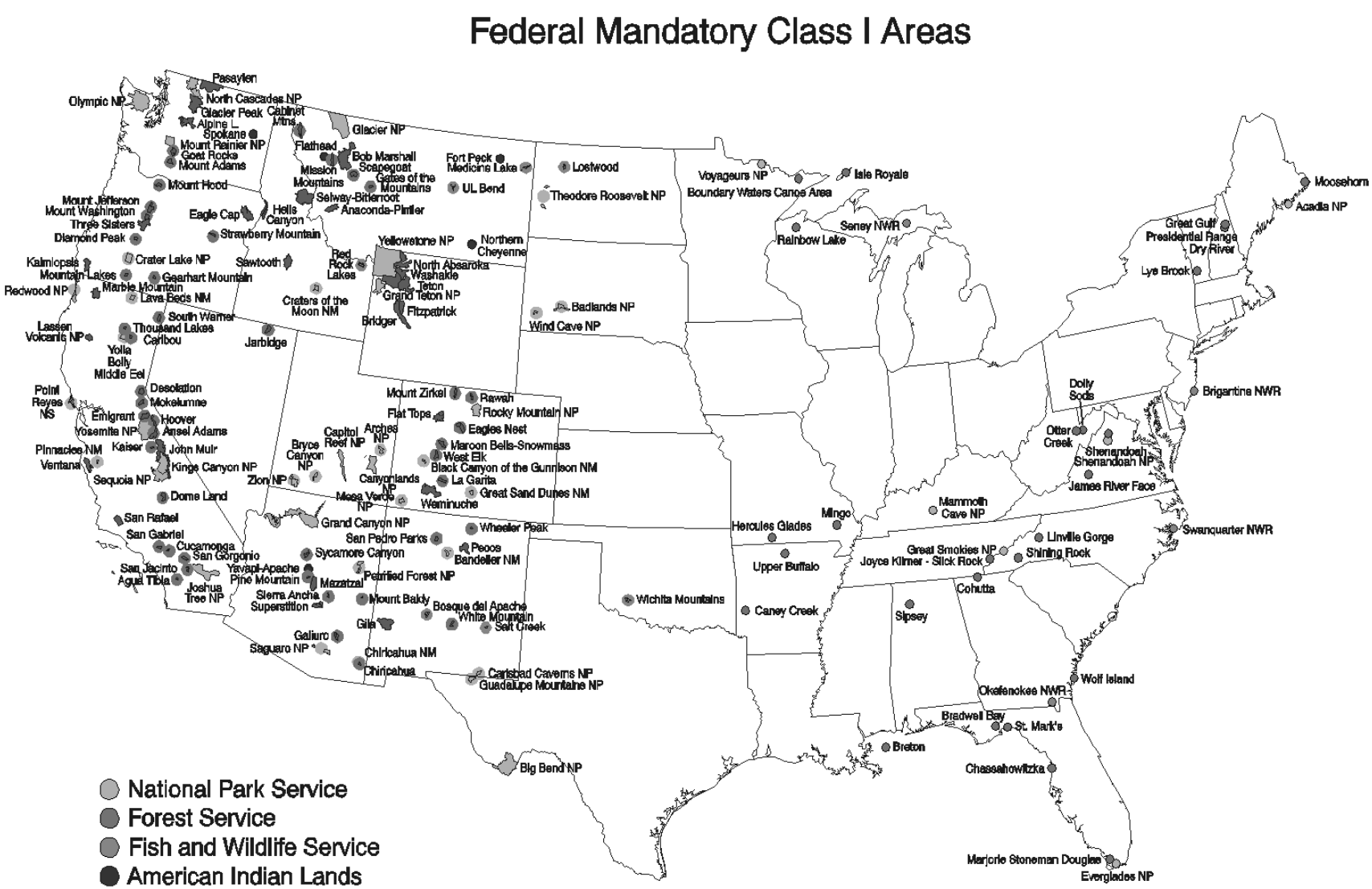

Figure 1.1. Class I areas of the contiguous United States. The shade coding identifies the managing agency of each Class I area.

1.2 OVERVIEW OF THE IMPROVE MONITORING NETWORK

1.2.1 Site Location

The IMPROVE network initially consisted of 30 monitoring sites in CIAs: twenty of these sites began operation in 1987, followed by the others in the early 1990s. An additional ~40 sites, most in remote areas, that used the same instrumentation, monitoring, and analysis protocols (called IMPROVE protocol sites) began operation prior to 2000 and were separately sponsored by individual federal or state organizations, though they were operated identically to other sites in the IMPROVE network. Adjustments to the number of monitoring sites in the network or the suite of measurements collected at an individual site occurred on several occasions, due in some cases to scientific considerations and in others to resource and funding limitations. Many of the sites also included optical monitoring with a nephelometer, a transmissometer, and/or color photography to document scenic appearance. The optical monitoring sites are detailed below in section 1.2.3.

In 1998 the EPA increased its support of IMPROVE to expand the network in Class I areas to provide the monitoring required under the RHR. Details regarding the selection process of additional sites was provided in the third IMPROVE report (Malm et al., 2000). The selection process was completed by the end of 1999 and installations began shortly thereafter. Currently the network consists of 212 sites (170 operating and 42 discontinued), including representative sites for the CIAs, and additional sites to fill in the spatial gaps where CIAs are sparse or absent. A list of sampling sites is provided in Table 1.1, including the site name, site code, state, latitude, longitude, elevation, and dates of operation. The sites are grouped by region, an empirical categorization that organizes sites with similar aerosol species and concentrations by location. Class I areas and their representative sites are listed in Table 1.2. A map of the site locations is provided in Figure 1.2, including IMPROVE and IMPROVE protocol sites. The sites are depicted by their site code and shaded based on their region, as defined in Table 1.1. There are 41 IMPROVE regions, 28 of which are rural and an additional thirteen that correspond to a single urban site per region (listed individually under “Urban Quality Assurance Sites” in Table 1.1). Of the rural sites, four regions include only one site (Death Valley, Lone Peak, Virgin Islands, and Ontario).

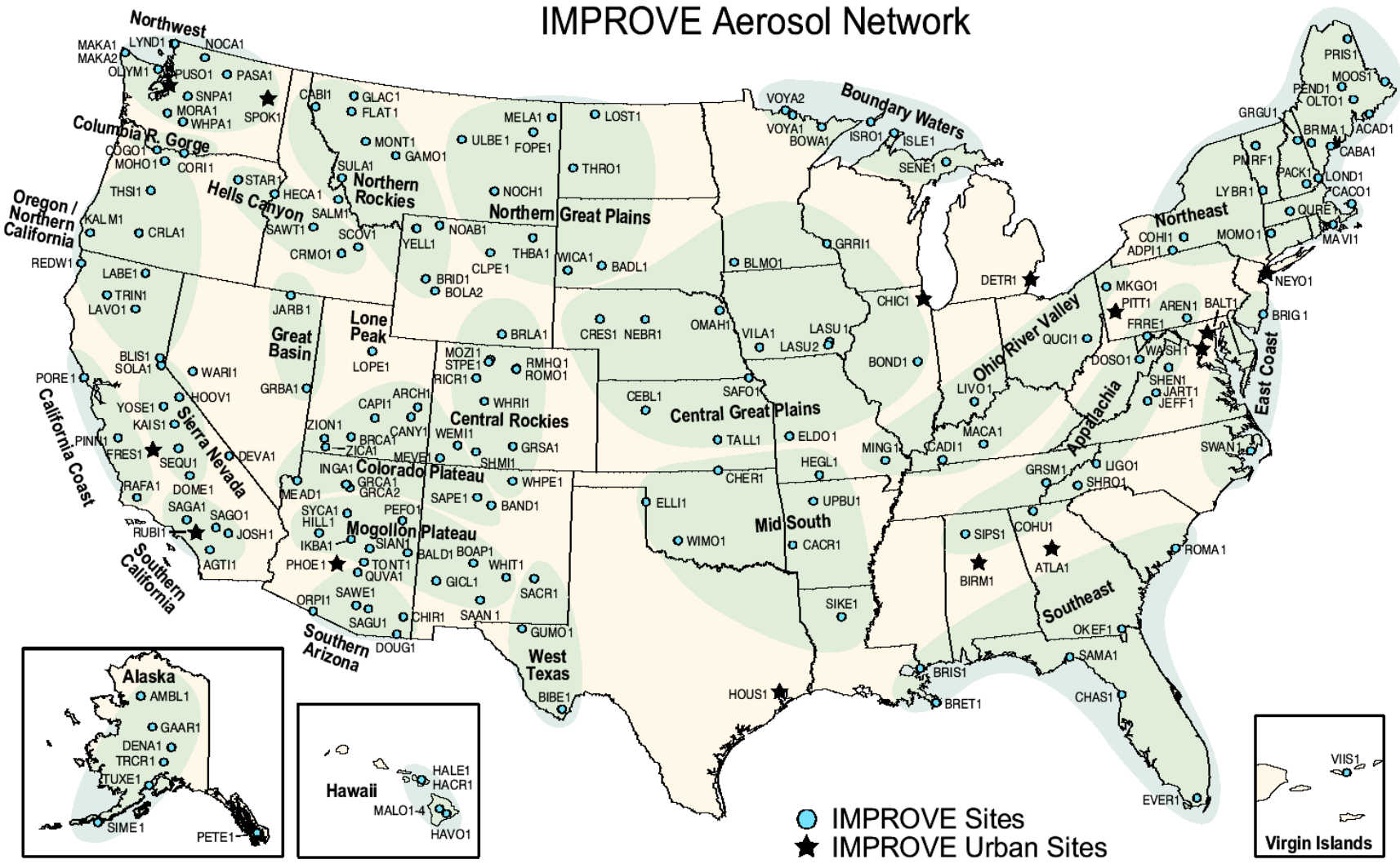

Figure 1.2. Locations of IMPROVE and IMPROVE protocol sites are shown for all discontinued and current sites as of December 2010. The IMPROVE regions used for grouping the sites are indicated by shading and bold text. Urban sites included in the IMPROVE network for quality assurance purposes are identified by stars.

Table 1.1. Currently operating and discontinued IMPROVE particulate monitoring sites. The sites are grouped by region, as displayed in Figure 1.2.

Site Name	Site Code	State	Latitude	Longitude	Elevation (m)	Dates of Operation
Alaska						
Ambler	AMBL1	AK	67.099	-157.872	67	07/2004-08/2005
Denali NP	DENA1	AK	63.723	-148.968	675	03/1988-present
Gates of the Arctic	GAAR1	AK	66.931	-151.492	205	10/2008-present
Petersburg	PETE1	AK	56.611	-132.812	12	07/2004-09/2009
Simeonof	SIME1	AK	55.325	-160.506	57	09/2001-present
Trapper Creek	TRCR1	AK	62.315	-150.316	155	09/2001-present
Tuxedni	TUXE1	AK	59.992	-152.666	15	12/2001-present
Alberta						
Barrier Lake	BALA1	AB	51.029	-115.034	1391	01/2011-present
Appalachia						
Arendtsville	AREN1	PA	39.923	-77.308	267	04/2001-12/2010
Cohutta	COHU1	GA	34.785	-84.626	735	05/2000-present
Dolly Sods WA	DOSO1	WV	39.105	-79.426	1182	09/1991-present
Frostburg	FRRE1	MD	39.706	-79.012	767	04/2004-present
Great Smoky Mountains NP	GRSM1	TN	35.633	-83.942	811	03/1988-present
James River Face Wilderness	JARI1	VA	37.627	-79.513	290	06/2000-present
Jefferson NF	JEFF1	VA	37.617	-79.483	219	09/1994-05/2000
Linville Gorge	LIGO1	NC	35.972	-81.933	969	03/2000-present
Shenandoah NP	SHEN1	VA	38.523	-78.435	1079	03/1988-present
Shining Rock WA	SHRO1	NC	35.394	-82.774	1617	07/1994-present
Sipsy Wilderness	SIPS1	AL	34.343	-87.339	286	03/1992-present
Boundary Waters						
Boundary Waters Canoe Area	BOWA1	MN	47.947	-91.496	527	08/1991-present
Isle Royale NP	ISLE1	MI	47.46	-88.149	182	11/1999-present
Isle Royale NP	ISRO1	MI	47.917	-89.15	213	06/1988-07/1991
Seney	SENE1	MI	46.289	-85.95	215	11/1999-present
Voyageurs NP #1	VOYA1	MN	48.413	-92.83	426	03/1988-09/1996
Voyageurs NP #2	VOYA2	MN	48.413	-92.829	429	11/1999-present
California Coast						
Pinnacles NM	PINN1	CA	36.483	-121.157	302	03/1988-present
Point Reyes National Seashore	PORE1	CA	38.122	-122.909	97	03/1988-present
San Rafael	RAFA1	CA	34.734	-120.007	957	02/2000-present
Central Great Plains						
Blue Mounds	BLMO1	MN	43.716	-96.191	473	07/2002-present
Bondville	BOND1	IL	40.052	-88.373	263	03/2001-present
Cedar Bluff	CEBL1	KS	38.77	-99.763	666	06/2002-present
Crescent Lake	CRES1	NE	41.763	-102.434	1207	07/2002-present

Site Name	Site Code	State	Latitude	Longitude	Elevation (m)	Dates of Operation
El Dorado Springs	ELDO1	MO	37.701	-94.035	298	06/2002-present
Great River Bluffs	GRRI1	MN	43.937	-91.405	370	07/2002-present
Lake Sugema	LASU1	IA	40.688	-91.988	223	06/2002-11/2004
Lake Sugema	LASU2	IA	40.693	-92.006	229	12/2004-present
Nebraska NF	NEBR1	NE	41.889	-100.339	883	07/2002-present
Omaha	OMAH1	NE	42.149	-96.432	430	08/2003-08/2008
Sac and Fox	SAFO1	KS	39.979	-95.568	293	06/2002-present
Tallgrass	TALL1	KS	38.434	-96.56	390	09/2002-present
Viking Lake	VILA1	IA	40.969	-95.045	371	06/2002-present
Central Rocky Mountains						
Brooklyn Lake	BRLA1	WY	41.365	-106.240	3196	09/1993-12/2003
Great Sand Dunes NM	GRSA1	CO	37.725	-105.519	2498	05/1988-present
Mount Zirkel WA	MOZI1	CO	40.538	-106.677	3243	07/1994-present
Ripple Creek	RICR1	CO	40.085	-107.312	2934	02/2009-present
Rocky Mountain NP HQ	RMHQ1	CO	40.362	-105.564	2408	03/1988-02/1991
Rocky Mountain NP	ROMO1	CO	40.278	-105.546	2760	09/1990-present
Storm Peak	STPE1	CO	40.445	-106.74	3220	12/1993-07/1994
Shamrock Mine	SHMI1	CO	37.303	-107.484	2351	7/2004-present
Wheeler Peak	WHPE1	NM	36.585	-105.452	3366	08/2000-present
White River NF	WHRI1	CO	39.154	-106.821	3414	07/1993-present
Colorado Plateau						
Arches NP	ARCH1	UT	38.783	-109.583	1722	03/1988-05/1992
Bandelier NM	BAND1	NM	35.78	-106.266	1988	03/1988-present
Bryce Canyon NP	BRCA1	UT	37.618	-112.174	2481	03/1988-present
Canyonlands NP	CANY1	UT	38.459	-109.821	1798	03/1988-present
Capitol Reef NP	CAPI1	UT	38.302	-111.293	1897	03/2000-present
Hopi Point #1	GRCA1	AZ	36.066	-112.154	2164	03/1988-08/1998
Hance Camp at Grand Canyon NP	GRCA2	AZ	35.973	-111.984	2267	09/1997-present
Indian Gardens	INGA1	AZ	36.078	-112.129	1166	10/1989-present
Meadview	MEAD1	AZ	36.019	-114.068	902	09/1991-09/1992 02/2003-present
Mesa Verde NP	MEVE1	CO	37.198	-108.491	2172	03/1988-present
San Pedro Parks	SAPE1	NM	36.014	-106.845	2935	08/2000-present
Weminuche WA	WEMI1	CO	37.659	-107.8	2750	03/1988-present
Zion Canyon	ZICA1	UT	37.198	-113.151	1215	12/2002-present
Zion	ZION1	UT	37.459	-113.224	1545	03/2000-08/2004
Columbia River Gorge						

Site Name	Site Code	State	Latitude	Longitude	Elevation (m)	Dates of Operation
Columbia Gorge #1	COGO1	WA	45.569	-122.21	230	09/1996-present
Columbia River Gorge	CORI1	WA	45.664	-121.001	179	06/1993-present
Death Valley						
Death Valley NP	DEVA1	CA	36.509	-116.848	130	10/1993-present
East Coast						
Brigantine NWR	BRIG1	NJ	39.465	-74.449	5	09/1991-present
Swanquarter	SWAN1	NC	35.451	-76.207	-4	06/2000-present
Great Basin						
Great Basin NP	GRBA1	NV	39.005	-114.216	2066	05/1992-present
Jarbidge WA	JARB1	NV	41.893	-115.426	1869	03/1988-present
Hawaii						
Haleakala Crater NP	HACR1	HI	20.759	-156.248	2158	01/2007-present
Haleakala NP	HALE1	HI	20.809	-156.282	1153	02/1991-present
Hawaii Volcanoes NP	HAVO1	HI	19.431	-155.258	1259	03/1988-present
Mauna Loa Observatory #1	MALO1	HI	19.536	-155.577	3439	03/1995-present
Mauna Loa Observatory #2	MALO2	HI	19.536	-155.577	3439	03/1995-present
Mauna Loa Observatory #3	MALO3	HI	19.539	-155.578	3400	04/1996-05/1996
Mauna Loa Observatory #4	MALO4	HI	19.539	-155.578	3400	04/1996-05/1996
Hells Canyon						
Craters of the Moon NM	CRMO1	ID	43.461	-113.555	1818	05/1992-present
Hells Canyon	HECA1	OR	44.97	-116.844	655	08/2000-present
Sawtooth NF	SAWT1	ID	44.17	-114.927	1990	01/1994-present
Scoville	SCOV1	ID	43.65	-113.033	1500	05/1992-05/1997
Starkey	STAR1	OR	45.225	-118.513	1259	03/2000-present
Lone Peak						
Lone Peak WA	LOPE1	UT	40.445	-111.708	1768	12/1993-08/2001
Mid South						
Caney Creek	CACR1	AR	34.454	-94.143	683	06/2000-present
Cherokee Nation	CHER1	OK	36.956	-97.031	342	09/2002-present
Ellis	ELLI1	OK	36.085	-99.935	697	06/2002-present
Hercules-Glades	HEGL1	MO	36.614	-92.922	404	03/2001-present
Sikes	SIKE1	LA	32.057	-92.435	45	03/2001-12/2010
Upper Buffalo WA	UPBU1	AR	35.826	-93.203	723	12/1991-present
Wichita Mountains	WIMO1	OK	34.732	-98.713	509	03/2001-present
Mogollon Plateau						
Mount Baldy	BALD1	AZ	34.058	-109.441	2509	02/2000-present

Site Name	Site Code	State	Latitude	Longitude	Elevation (m)	Dates of Operation
Bosque del Apache	BOAP1	NM	33.87	-106.852	1390	04/2000-present
Gila WA	GICL1	NM	33.22	-108.235	1776	04/1994-present
Hillside	HILL1	AZ	34.429	-112.963	1511	04/2001-06/2005
Ike's Backbone	IKBA1	AZ	34.34	-111.683	1298	04/2000-present
Petrified Forest NP	PEFO1	AZ	35.078	-109.769	1766	03/1988-present
San Andres	SAAN1	NM	32.687	-106.484	1326	10/1997-08/2000
Sierra Ancha	SIAN1	AZ	34.091	-110.942	1600	02/2000-present
Sycamore Canyon	SYCA1	AZ	35.141	-111.969	2046	09/1991-present
Tonto NM	TONT1	AZ	33.655	-111.107	775	04/1988-present
White Mountain	WHIT1	NM	33.469	-105.535	2064	01/2002-present
Northeast						
Acadia NP	ACAD1	ME	44.377	-68.261	157	03/1988-present
Addison Pinnacle	ADPI1	NY	42.091	-77.21	512	04/2001-06/2010
Bridgton	BRMA1	ME	44.107	-70.729	234	03/2001-present
Casco Bay	CABA1	ME	43.833	-70.064	27	03/2001-present
Cape Cod	CACO1	MA	41.976	-70.024	49	04/2001-present
Connecticut Hill	COHI1	NY	42.401	-76.653	519	04/2001-07/2006
Great Gulf WA	GRGU1	NH	44.308	-71.218	454	06/1995-present
Londonderry	LOND1	NH	42.862	-71.380	124	12/2010-present
Lye Brook WA	LYBR1	VT	43.148	-73.127	1015	09/1991-present
Martha's Vineyard	MAVI1	MA	41.331	-70.785	3	01/2003-present
Mohawk Mt.	MOMO1	CT	41.821	-73.297	522	09/2001-present
Moosehorn NWR	MOOS1	ME	45.126	-67.266	78	12/1994-present
Old Town	OLTO1	ME	44.933	-68.646	51	07/2001-06/2006
Pack Monadnock Summit	PACK1	NH	42.862	-71.879	695	10/2007-present
Penobscot	PENO1	ME	44.948	-68.648	45	1/2006-present
Proctor Maple Research Facility	PMRF1	VT	44.528	-72.869	401	12/1993-present
Presque Isle	PRIS1	ME	46.696	-68.033	166	03/2001-present
Quabbin Summit	QURE1	MA	42.298	-72.335	318	03/2001-present
Northern Great Plains						
Badlands NP	BADL1	SD	43.743	-101.941	736	03/1988-present
Cloud Peak	CLPE1	WY	44.334	-106.957	2471	06/2002-present
Fort Peck	FOPE1	MT	48.308	-105.102	638	06/2002-present
Lostwood	LOST1	ND	48.642	-102.402	696	12/1999-present
Medicine Lake	MELA1	MT	48.487	-104.476	606	12/1999-present
Northern Cheyenne	NOCH1	MT	45.65	-106.557	1283	06/2002-present
Thunder Basin	THBA1	WY	44.663	-105.287	1195	06/2002-present

Site Name	Site Code	State	Latitude	Longitude	Elevation (m)	Dates of Operation
Theodore Roosevelt	THRO1	ND	46.895	-103.378	853	12/1999-present
UL Bend	ULBE1	MT	47.582	-108.72	891	01/2000-present
Wind Cave	WICA1	SD	43.558	-103.484	1296	12/1999-present
Northern Rocky Mountains						
Boulder Lake	BOLA1	WY	42.846	-109.640	2296	10/2009-present
Bridger WA	BRID1	WY	42.975	-109.758	2627	03/1988-present
Cabinet Mountains	CABI1	MT	47.955	-115.671	1441	07/2000-present
Flathead	FLAT1	MT	47.773	-114.269	1580	06/2002-present
Gates of the Mountains	GAMO1	MT	46.826	-111.711	2387	07/2000-present
Glacier NP	GLAC1	MT	48.511	-113.997	975	03/1988-present
Monture	MONT1	MT	47.122	-113.154	1282	03/2000-present
North Absaroka	NOAB1	WY	44.745	-109.382	2483	01/2000-present
Salmon NF	SALM1	ID	45.159	-114.026	2788	12/1993-08/2000
Sula Peak	SULA1	MT	45.86	-114	1896	08/1994-present
Yellowstone NP 1	YELL1	WY	44.565	-110.4	2442	03/1988-07/1996
Yellowstone NP 2	YELL2	WY	44.565	-110.4	2425	07/1996-present
Northwest						
Lynden	LYND1	WA	48.953	-122.559	28	10/1996-08/1997
Makah Indian Reservation	MAKA1	WA	48.372	-124.595	9	9/2006-10/2010
Makah Indian Reservation	MAKA2	WA	48.298	-124.625	480	10/2010-present
Mount Rainier NP	MORA1	WA	46.758	-122.124	439	03/1988-present
North Cascades	NOCA1	WA	48.732	-121.065	569	03/2000-present
Olympic	OLYM1	WA	48.007	-122.973	600	07/2001-present
Pasayten	PASA1	WA	48.388	-119.927	1627	11/2000-present
Snoqualmie Pass	SNPA1	WA	47.422	-121.426	1049	07/1993-present
Spokane Res.	SPOK1	WA	47.904	-117.861	552	07/2001-06/2005
White Pass	WHPA1	WA	46.624	-121.388	1827	02/2000-present
Not Assigned						
Walker River Paiute Tribe	WARI1	NV	38.952	-118.815	1250	06/2003-11/2005
Ohio River Valley						
Cadiz	CADI1	KY	36.784	-87.85	192	03/2001-12/2010
Livonia	LIVO1	IN	38.535	-86.26	282	03/2001-12/2010
Mammoth Cave NP	MACA1	KY	37.132	-86.148	235	09/1991-present
Mingo	MING1	MO	36.972	-90.143	111	05/2000-present
M.K. Goddard	MKGO1	PA	41.427	-80.145	380	04/2001-12/2010
Quaker City	QUCI1	OH	39.943	-81.338	366	05/2001-present
Ontario						
Egbert	EGBE1		44.231	-79.783	251	5/2005-present
Oregon and Northern California						
Bliss SP (TRPA)	BLIS1	CA	38.976	-120.103	2131	11/1990-present

Site Name	Site Code	State	Latitude	Longitude	Elevation (m)	Dates of Operation
Crater Lake NP	CRLA1	OR	42.896	-122.136	1996	03/1988-present
Kalmiopsis	KALM1	OR	42.552	-124.059	80	03/2000-present
Lava Beds NM	LABE1	CA	41.712	-121.507	1460	03/2000-present
Lassen Volcanic NP	LAVO1	CA	40.54	-121.577	1733	03/1988-present
Mount Hood	MOHO1	OR	45.289	-121.784	1531	03/2000-present
Redwood NP	REDW1	CA	41.561	-124.084	244	03/1988-present
Three Sisters WA	THSI1	OR	44.291	-122.043	885	07/1993-present
Trinity	TRIN1	CA	40.786	-122.805	1014	07/2000-present
Phoenix						
Phoenix	PHOE1	AZ	33.504	-112.096	342	04/2001-present
Puget Sound						
Puget Sound	PUSO1	WA	47.57	-122.312	98	03/1996-present
Sierra Nevada						
Dome Lands WA	DOLA1	CA	35.699	-118.202	914	08/1994-10/1998
Dome Lands WA	DOME1	CA	35.728	-118.138	927	02/2000-present
Hoover	HOOV1	CA	38.088	-119.177	2561	07/2001-present
Kaiser	KAIS1	CA	37.221	-119.155	2598	01/2000-present
Sequoia NP	SEQU1	CA	36.489	-118.829	519	03/1992-present
South Lake Tahoe	SOLA1	CA	38.933	-119.967	1900	03/1989-06/1997
Yosemite NP	YOSE1	CA	37.713	-119.706	1603	03/1988-present
Southeast						
Breton	BRET1	LA	29.119	-89.207	11	06/2000-09/2005
Breton Island	BRIS1	LA	30.109	-89.762	-7	01/2008-present
Chassahowitzka NWR	CHAS1	FL	28.748	-82.555	4	04/1993-present
Everglades NP	EVER1	FL	25.391	-80.681	1	09/1988-present
Okefenokee NWR	OKEF1	GA	30.741	-82.128	48	09/1991-present
Cape Romain NWR	ROMA1	SC	32.941	-79.657	5	09/1994-present
St. Marks	SAMA1	FL	30.093	-84.161	8	06/2000-present
Southern Arizona						
Chiricahua NM	CHIR1	AZ	32.009	-109.389	1555	03/1988-present
Douglas	DOUG1	AZ	31.349	-109.54	1230	06/2004-present
Organ Pipe	ORPI1	AZ	31.951	-112.802	504	01/2003-present
Queen Valley	QUVA1	AZ	33.294	-111.286	661	04/2001-present
Saguaro NM	SAGU1	AZ	32.175	-110.737	941	06/1988-present
Saguaro West	SAWE1	AZ	32.249	-111.218	714	04/2001-present
Southern California						
Agua Tibia	AGTI1	CA	33.464	-116.971	508	11/2000-present
Joshua Tree NP	JOSH1	CA	34.069	-116.389	1235	02/2000-present
Joshua Tree NP	JOTR1	CA	34.069	-116.389	1228	09/1991-07/1992
San Gabriel	SAGA1	CA	34.297	-118.028	1791	12/2000-present
San Gorgonio WA	SAGO1	CA	34.194	-116.913	1726	03/1988-present
Urban Quality Assurance Sites						
Atlanta	ATLA1	GA	33.688	-84.29	243	04/2004-present

Site Name	Site Code	State	Latitude	Longitude	Elevation (m)	Dates of Operation
Baltimore	BALT1	MD	39.255	-76.709	78	06/2004-02/2007
Birmingham	BIRM1	AL	33.553	-86.815	176	04/2004-present
Chicago	CHIC1	IL	41.751	-87.713	195	11/2003-09/2005
Detroit	DETR1	MI	42.229	-83.209	180	11/2003-present
Fresno	FRES1	CA	36.782	-119.773	100	09/2004-present
Houston	HOUS1	TX	29.67	-95.129	7	05/2004-09/2005
New York City	NEYO1	NY	40.816	-73.902	45	08/2004-04/2010
Pittsburgh	PITT1	PA	40.465	-79.961	268	04/2004-present
Rubidoux	RUBI1	CA	34	-117.416	248	09/2004-09/2005
Virgin Islands						
Virgin Islands NP	VIIS1	VI	18.336	-64.796	51	10/1990-present
Washington D.C.						
Washington D.C.	WASH1	DC	38.876	-77.034	15	03/1988-present
West Texas						
Big Bend NP	BIBE1	TX	29.303	-103.178	1067	03/1988-present
Guadalupe Mountains NP	GUMO1	TX	31.833	-104.809	1672	03/1988-present
Salt Creek	SACR1	NM	33.46	-104.404	1072	04/2000-present

NF = National Forest
NM = National Monument
NP = National Park
NWR = National Wildlife Refuge
WA = Wilderness Area

Table 1.2. Class I areas and the representative monitoring site.

Class I Area Name	Site Name	Site Code
Acadia	Acadia NP	ACAD1
Agua Tibia	Agua Tibia	AGTI1
Alpine Lakes	Snoqualmie Pass	SNPA1
Anaconda-Pintler	Sula Peak	SULA1
Ansel Adams	Kaiser	KAIS1
Arches	Canyonlands NP	CANY1
Badlands	Badlands NP	BADL1
Bandelier	Bandelier NM	BAND1
Big Bend	Big Bend NP	BIBE1
Black Canyon of the Gunnison	Weminuche WA	WEMI1
Bob Marshall	Monture	MONT1
Bosque del Apache	Bosque del Apache	BOAP1
Boundary Waters Canoe Area	Boundary Waters Canoe Area	BOWA1
Breton	Breton	BRIS1
Bridger	Bridger WA	BRID1
Brigantine	Brigantine NWR	BRIG1
Bryce Canyon	Bryce Canyon NP	BRCA1
Cabinet Mountains	Cabinet Mountains	CABI1
Caney Creek	Caney Creek	CACR1
Canyonlands	Canyonlands NP	CANY1
Cape Romain	Cape Romain NWR	ROMA1
Capitol Reef	Capitol Reef NP	CAPI1
Caribou	Lassen Volcanic NP	LAVO1
Carlsbad Caverns	Guadalupe Mountains NP	GUMO1

Class I Area Name	Site Name	Site Code
Chassahowitzka	Chassahowitzka NWR	CHAS1
Chiricahua NM	Chiricahua NM	CHIR1
Chiricahua W	Chiricahua NM	CHIR1
Cohutta	Cohutta	COHU1
Crater Lake	Crater Lake NP	CRLA1
Craters of the Moon	Craters of the Moon NM	CRMO1
Cucamonga	San Gabriel	SAGA1
Denali	Denali NP	DENA1
Desolation	Bliss SP (TRPA)	BLIS1
Diamond Peak	Crater Lake NP	CRLA1
Dolly Sods	Dolly Sods WA	DOSO1
Dome Land	Dome Lands WA	DOME1
Eagle Cap	Starkey	STAR1
Eagles Nest	White River NF	WHRI1
Emigrant	Yosemite NP	YOSE1
Everglades	Everglades NP	EVER1
Fitzpatrick	Bridger WA	BRID1
Flat Tops	White River NF	WHRI1
Galiuro	Chiricahua NM	CHIR1
Gates of the Mountains	Gates of the Mountains	GAMO1
Gearhart Mountain	Crater Lake NP	CRLA1
Gila	Gila WA	GICL1
Glacier	Glacier NP	GLAC1
Glacier Peak	North Cascades	NOCA1
Goat Rocks	White Pass	WHPA1
Grand Canyon	Hance Camp at Grand Canyon NP	GRCA2
Grand Teton	Yellowstone NP 2	YELL2
Great Gulf	Great Gulf WA	GRGU1
Great Sand Dunes	Great Sand Dunes NM	GRSA1
Great Smoky Mountains	Great Smoky Mountains NP	GRSM1
Guadalupe Mountains	Guadalupe Mountains NP	GUMO1
Haleakala	Haleakala NP	HALE1
Hawaii Volcanoes	Hawaii Volcanoes NP	HAVO1
Hells Canyon	Hells Canyon	HECA1
Hercules-Glade	Hercules-Glades	HEGL1
Hoover	Hoover	HOOV1
Isle Royale	Isle Royale NP	ISLE1
James River Face	James River Face WA	JARI1
Jarbidge	Jarbidge WA	JARB1
John Muir	Kaiser	KAIS1
Joshua Tree	Joshua Tree NP	JOSH1
Joyce Kilmer-Slickrock	Great Smoky Mountains NP	GRSM1
Kaiser	Kaiser	KAIS1
Kalmiopsis	Kalmiopsis	KALM1
Kings Canyon	Sequoia NP	SEQU1
La Garita	Weminuche WA	WEMI1
Lassen Volcanic	Lassen Volcanic NP	LAVO1
Lava Beds	Lava Beds NM	LABE1
Linville Gorge	Linville Gorge	LIGO1
Lostwood	Lostwood	LOST1
Lye Brook	Lye Brook WA	LYBR1
Mammoth Cave	Mammoth Cave NP	MACA1

Class I Area Name	Site Name	Site Code
Marble Mountain	Trinity	TRIN1
Maroon Bells-Snowmass	White River NF	WHRI1
Mazatzal	Ike's Backbone	IKBA1
Medicine Lake	Medicine Lake	MELA1
Mesa Verde	Mesa Verde NP	MEVE1
Mingo	Mingo	MING1
Mission Mountains	Monture	MONT1
Mokelumne	Bliss SP (TRPA)	BLIS1
Moosehorn	Moosehorn NWR	MOOS1
Mount Adams	White Pass	WHPA1
Mount Baldy	Mount Baldy	BALD1
Mount Hood	Mount Hood	MOHO1
Mount Jefferson	Three Sisters WA	THSI1
Mount Rainier	Mount Rainier NP	MORA1
Mount Washington	Three Sisters WA	THSI1
Mount Zirkel	Mount Zirkel WA	MOZI1
Mountain Lakes	Crater Lake NP	CRLA1
North Absaroka	North Absaroka	NOAB1
North Cascades	North Cascades	NOCA1
Okefenokee	Okefenokee NWR	OKEF1
Olympic	Olympic	OLYM1
Otter Creek	Dolly Sods WA	DOSO1
Pasayten	Pasayten	PASA1
Pecos	Wheeler Peak	WHPE1
Petrified Forest	Petrified Forest NP	PEFO1
Pine Mountain	Ike's Backbone	IKBA1
Pinnacles	Pinnacles NM	PINN1
Point Reyes	Point Reyes National Seashore	PORE1
Presidential Range-Dry River	Great Gulf WA	GRGU1
Rawah	Mount Zirkel WA	MOZI1
Red Rock Lakes	Yellowstone NP 2	YELL2
Redwood	Redwood NP	REDW1
Rocky Mountain	Rocky Mountain NP	ROMO1
Roosevelt Campobello	Moosehorn NWR	MOOS1
Saguaro	Saguaro NM	SAGU1
Saint Marks	St. Marks	SAMA1
Salt Creek	Salt Creek	SACR1
San Gabriel	San Gabriel	SAGA1
San Gorgonio	San Gorgonio WA	SAGO1
San Jacinto	San Gorgonio WA	SAGO1
San Pedro Parks	San Pedro Parks	SAPE1
San Rafael	San Rafael	RAFA1
Sawtooth	Sawtooth NF	SAWT1
Scapegoat	Monture	MONT1
Selway-Bitterroot	Sula Peak	SULA1
Seney	Seney	SENE1
Sequoia	Sequoia NP	SEQU1
Shenandoah	Shenandoah NP	SHEN1
Shining Rock	Shining Rock WA	SHRO1
Sierra Ancha	Sierra Ancha	SIAN1
Simeonof	Simeonof	SIME1
Sipsey	Sipsy WA	SIPS1

Class I Area Name	Site Name	Site Code
South Warner	Lava Beds NM	LABE1
Strawberry Mountain	Starkey	STAR1
Superstition	Tonto NM	TONT1
Swanquarter	Swanquarter	SWAN1
Sycamore Canyon	Sycamore Canyon	SYCA1
Teton	Yellowstone NP 2	YELL2
Theodore Roosevelt	Theodore Roosevelt	THRO1
Thousand Lakes	Lassen Volcanic NP	LAVO1
Three Sisters	Three Sisters WA	THSI1
Tuxedni	Tuxedni	TUXE1
UL Bend	UL Bend	ULBE1
Upper Buffalo	Upper Buffalo WA	UPBU1
Ventana	Pinnacles NM	PINN1
Virgin Islands	Virgin Islands NP	VIIS1
Voyageurs	Voyageurs NP #2	VOYA2
Washakie	North Absaroka	NOAB1
Weminuche	Weminuche WA	WEMI1
West Elk	White River NF	WHRI1
Wheeler Peak	Wheeler Peak	WHPE1
White Mountain	White Mountain	WHIT1
Wichita Mountains	Wichita Mountains	WIMO1
Wind Cave	Wind Cave	WICA1
Wolf Island	Okefenokee NWR	OKEF1
Yellowstone	Yellowstone NP 2	YELL2
Yolla Bolly-Middle Eel	Trinity	TRIN1
Yosemite	Yosemite NP	YOSE1
Zion	Zion	ZION1

NF = National Forest
NM = National Monument
NP = National Park
NWR = National Wildlife Refuge
WA = Wilderness Area

1.2.2 Aerosol Sampling and Analysis

The current configuration of the IMPROVE monitor collects 24-hour samples every third day. As previous reports have detailed, the samplers have undergone modifications over time (Malm et al., 2000; Debell et al., 2006). The version II sampler began operating in November 1999 through early 2000 and is in use currently at all IMPROVE sites. The version II sampler was implemented to allow for protocol changes that occurred in 2000 with the expansion of the IMPROVE network and the need for consistency with the EPA's fine mass and fine speciation monitoring network. Specifically, the need for consistency with the EPA's sampling schedule. Other sampling configuration changes for IMPROVE occurred to ensure more consistency regarding data collection protocols (e.g., inlet height, filter collection time after sampling). Other differences between the networks were not addressed, such as shipping temperatures and the suite of analytes. Details regarding the version I sampler can be found in previous reports (e.g., Malm et al., 2000).

The IMPROVE samplers (versions I and II) consist of four independent modules (A, B, C, and D; see Figure 1.3). Each module incorporates a separate inlet, filter pack, and pump

assembly. Modules A, B, and C are equipped with a 2.5 µm cyclone that allows for sampling of particles with aerodynamic diameters less than 2.5 µm, while module D is fitted with a PM_{10} inlet to collect particles with aerodynamic diameters less than 10 µm. Each module contains a filter substrate specific to the analysis planned (Figure 1.3).

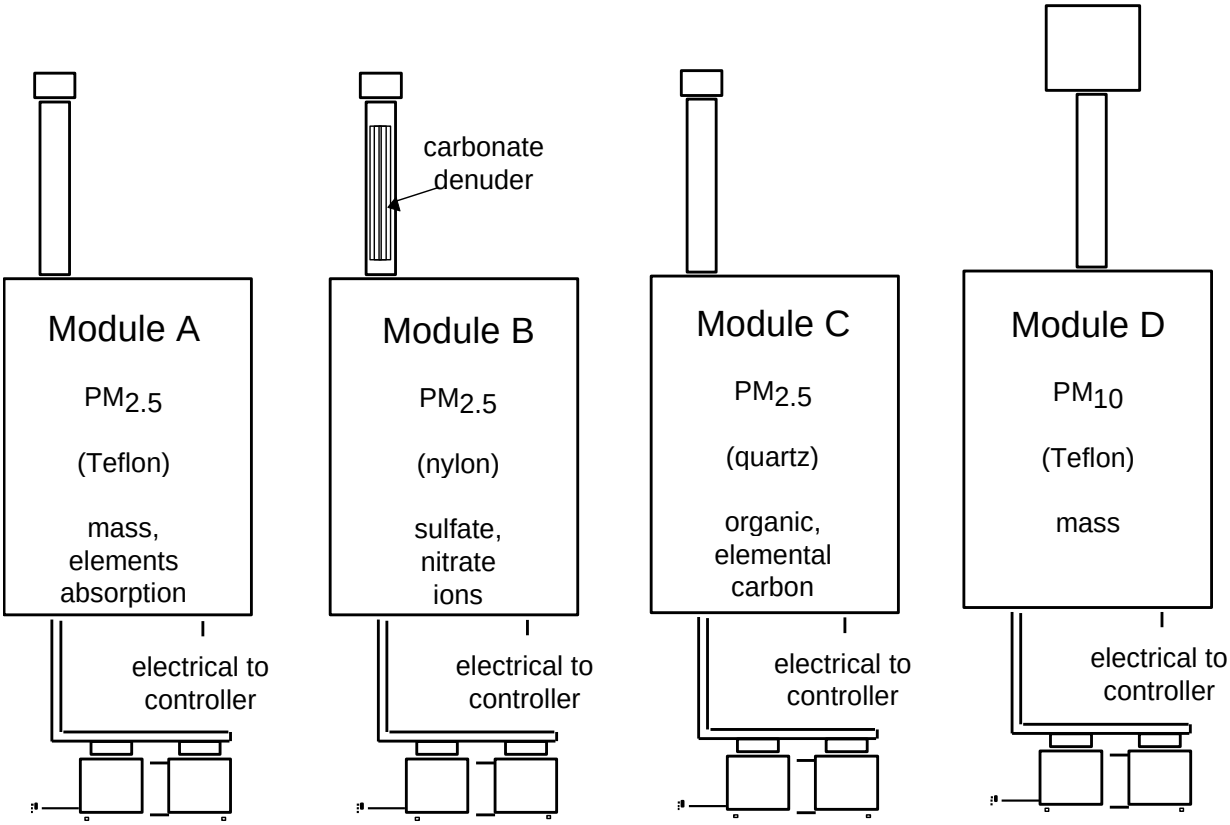

Figure 1.3. Schematic view of the IMPROVE sampler showing the four modules with separate inlets and pumps. The substrates with analyses performed for each module are also shown.

The version II sampler is controlled with a microprocessor programmed to maintain a given sampling schedule. Flow rate, sample temperature, and other performance-related information are recorded every 15 minutes throughout the sample period on a memory card reader/writer. The microprocessor also permits programming changes to be distributed to the controller on chips that are installed during annual maintenance visits, allowing for programming changes to be implemented consistently, without requiring programming in the field.

To accommodate the every-third-day sampling schedule, the version II sampler has a four-filter manifold for each module. The manifold with the solenoids sits directly above the filter cassettes and is raised or lowered as a unit to unload and load the filters. The four filter cassettes are held in a cartridge (shown in Figure 1.4) that is designed to allow only one orientation in the sampler. Fully prepared date- and site-labeled filter cartridges, along with memory cards, are sent from the analysis laboratory to the field and are returned in special mailing containers to prevent confusion concerning the order of sampling among the filters. If filter change service is performed on a sample day, the operator moves the cassette containing that day's filter to the open position in the newly loaded cartridge. The few minutes that it takes

to perform this sample change is recorded by the microprocessor on the memory card so that the correct air volume is used to calculate concentrations.

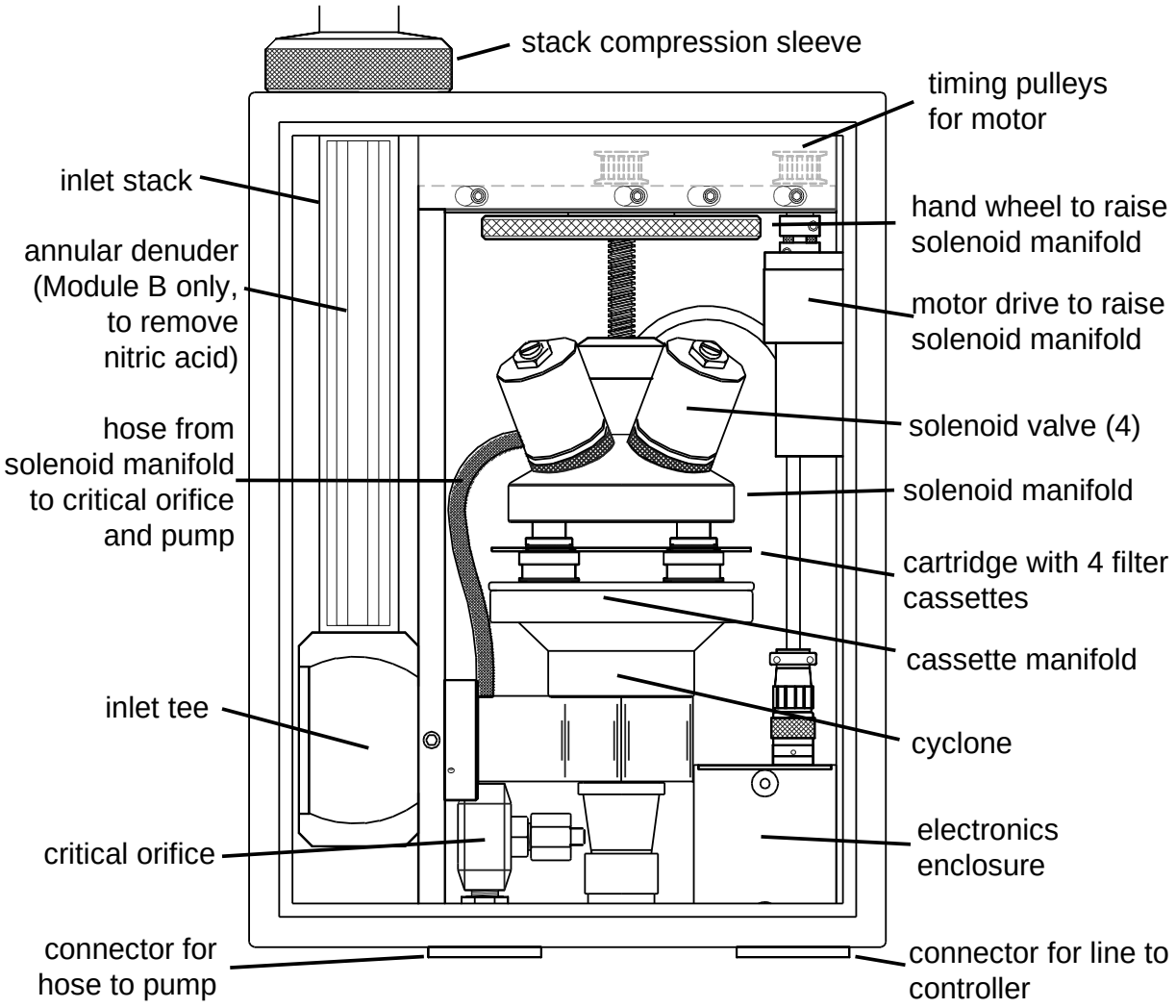

Figure 1.4. Schematic of the version II IMPROVE sampler $PM_{2.5}$ module.

The design of the version II IMPROVE sampler simplifies the addition of a fifth module to accommodate replicate sampling and analysis for mass and composition. This quality assurance module is operated for each sampling period and collects a replicate sample for one of the four modules (A, B, C, or D) so that, over time, relative precision information can be developed for each parameter. Starting in 2003, collocated modules were installed at 25 sites across the network, providing ~4% replication for each of the four modules (Table 1.3).

Table 1.3. Sites with a fifth collocated module.

Site Name	Site	A	B	C	D	Start Date	End Date
Mesa Verde NP	MEVE1	X				8/13/2003	
Olympic NP	OLYM1	X				11/8/2003	
Proctor Maple Research Facility	PMRF1	X				9/3/2003	
Sac and Fox	SAFO1	X				11/20/2003	
St. Marks	SAMA1	X				11/18/2004	

Site Name	Site	A	B	C	D	Start Date	End Date
Trapper Creek	TRCR1	X				6/22/2004	
Big Bend NP	BIBE1		X			8/30/2003	
Blue Mounds	BLMO1		X			9/16/2004	
Frostburg	FRRE1		X			4/15/2004	
Gates of the Mountains	GAMO1		X			9/23/2003	
Lassen Volcanic NP	LAVO1		X			4/18/2003	
Mammoth Cave NP	MACA1		X			5/12/2003	
Everglades NP	EVER1			X		7/11/2003	
Hercules-Glades	HEGL1			X		8/24/2004	
Hoover	HOOV1			X		8/13/2003	
Medicine Lake	MELA1			X		9/25/2003	
Saguaro West	SAWE1			X		3/25/2004	
Seney	SENE1			X		8/10/2003	
Houston	HOUS1				X	4/30/2004	9/1/2005
Jarbidge WA	JARB1				X	6/30/2004	
Joshua Tree NP	JOSH1				X	8/7/2003	
Quabbin Summit	QURE1				X	9/4/2003	
Swanquarter	SWAN1				X	11/9/2004	
Wind Cave	WICA1				X	9/17/2004	
Breton	BRIS1				X	1/28/2008	

NP = National Park
WA = Wilderness Area

The laboratory at University of California, Davis (UC Davis)[1] prepares the sample cartridges for the IMPROVE sites. Every 3 weeks, UC Davis sends a mailing container with the necessary sampling supplies to each site. The containers are typically received 10 days before the first sample-change day of the next 3-week cycle. Often there will be two containers at a site, one in current use and the second ready for the next period or ready to be shipped back to UC Davis. The site operators are expected to send the container with the exposed filters back to UC Davis within a day or two following the completion of each 3-week cycle. All shipments, to and from the field, are sent by second-day express delivery. Thus, a sample container typically spends a little over a month between shipment from and delivery to UC Davis, with the filters installed in the sampler during one week of that period.

As these filters arrive at UC Davis from the field sites, they are placed in Petri dishes and accumulate until a shipping tray has been filled, usually 400 filters. Nylon filters are sent to RTI (Research Triangle Institute)[2] for ion analysis and quartz filters are sent to DRI (Desert Research Institute)[3] for carbon analysis. Full trays of each type are sent to RTI and DRI approximately once a week by overnight express.

Module A is equipped with at Teflon® filter that is analyzed for $PM_{2.5}$ gravimetric fine mass, elemental analysis, and light absorption. Samples are pre- and post-weighed to gravimetrically determine $PM_{2.5}$ fine mass using electro-microbalance, after equilibrating at 30–40% relative humidity and 20–30° C. This procedure for determining gravimetric fine mass is associated with both positive and negative artifacts. Negative artifacts include loss of

[1] UC Davis is the NPS contractor during the time period of this report.
[2] RTI is the NPS contractor for the ion analyses during the time period of this report.
[3] DRI is the NPS contractor for the carbon analyses during the time period of this report.

semivolatile species such as ammonium nitrate (AN) and some organic species from the Teflon filter during sampling. Positive artifacts include particle-bound water associated with hygroscopic aerosol species such as sulfates, nitrates, sea salt, and perhaps some organic species. Reactions with atmospheric gases may also contribute to positive artifacts. Storage conditions and shipping conditions may also contribute to artifacts.

Elemental analysis is performed on the module A Teflon filters for elements with atomic number greater than 11 (Na) and less than 82 (Pb) by X-ray florescence (XRF). The techniques used for elemental analysis for the IMPROVE network have included proton elastic scattering analysis (PESA), proton induced X-ray emission (PIXE), and XRF. Elemental hydrogen is quantified using PESA. PIXE was used for quantifying nearly all elements with atomic number greater than 11 and less than 82. Beginning in 1992, however, analysis of heavier elements with atomic weights from 26 (Fe) to 82 (Pb) switched to XRF with a molybdenum (Mo) anode source. PIXE was discontinued in late 2001 and analysis of the lighter elements with Z from 11 (Na) to 25 (Mn) was changed from PIXE to XRF using a copper (Cu) anode source. Also, in late 2001, the analysis of Fe was changed from Mo anode XRF to Cu anode XRF. In both cases the change from PIXE to XRF provided lower minimum detection limits (MDL) for most elements of interest, as well as better sample preservation for reanalysis. The exceptions were Na, Mg, Al, and to a lesser extent Si, where the change to Cu XRF resulted in significantly increased MDL and uncertainty. The details on the transitions from PIXE to XRF are provided in section 1.3 below.

The light absorption coefficient (f_{abs}, Mm^{-1}) is determined from the channel A Teflon filter using a hybrid integrating plate/sphere system (HIPS) that involves the direct measurement of the absorption of a laser beam (wavelength of 633 nm) over the area of the sample. Prior to March 1, 1994, a laser integrating plate method (LIPM) was used.

Module B is fitted with a sodium carbonate denuder tube in the inlet to remove gaseous nitric acid in the air sample, followed by a Nylasorb (nylon) filter as the collection substrate. The material collected on the nylon filter is extracted ultrasonically in an aqueous solution that is subsequently analyzed for the anions sulfate, nitrate, nitrite, and chloride using ion chromatography. The negative artifact associated with the loss of nitrate on Teflon filters is not as critical for nylon filters, as they have been shown to be more effective at capturing and retaining nitrate from semivolatile AN than Teflon filters (Yu et al., 2005).

Field blanks for the B module are collected to determine positive artifacts that are used to correct concentrations of all the reported anions. A field blank nylon filter is placed in an unused port in the filter cassette where it is exposed to all aspects of the filter handling process, with the exception of sample air drawn being through it (McDade et al., 2004). Each site receives a nylon filter field blank every 2–3 months, on average, resulting in approximately 70 field blanks collected each month (McDade et al., 2004). A single artifact correction is applied for each species for every site in the network for the time period being processed. The artifact correction is calculated as the median of the filter blank values and subtracted from concentrations before they are reported. Monthly artifact corrections are computed currently, although prior to June 2002 seasonal quarters artifacts were applied. Sulfate ion artifacts are typically less than 10% of the ambient concentrations, and nitrate artifacts range between 10% and 20% for the filters used prior to 2004 (McDade et al., 2004). The filters introduced in 2004 were significantly cleaner,

with typical median blank values of 0.00 (below the MDL) for sulfate and nitrate and 0.01 $\mu g\ m^{-3}$ for chloride, approximately 100 times smaller than the chloride blank values observed prior to 2004.

Module C utilizes quartz fiber filters that are analyzed by thermal optical reflectance (TOR) for particulate organic and light absorbing carbon (OC and LAC, respectively) (Chow et al., 1993) and to estimate the organic carbon artifact from organic gases collected on the secondary filter. We use the term "light absorbing carbon" instead of elemental carbon (EC) to reflect the transition to this term in the scientific literature because of the operational definition, and sometimes morphology, associated with EC (Bond and Bergstrom, 2006; Malm et al., 1994). Light absorbing carbon particles may evolve in high temperature environments but not be graphitic (e.g., Hand et al., 2005). Replacing EC with LAC avoids potential confusion regarding the type of carbon particles responsible for light absorption.

Organic carbon concentrations reported by IMPROVE are corrected for an approximate positive artifact (Dillner et al., 2009). After-filters have been collected at six sites since 2001 (Chiricahua, Arizona, CHIR1; Grand Canyon, Arizona, GRCA2; Yosemite, California, YOSE1; Okefenokee, Georgia, OKEF1; Shenandoah, Virginia, SHEN1; and Mount Rainier, Washington, MORA1), and a monthly median artifact is used in a seasonal correction across the entire IMPROVE network (Watson et al., 2009; Chow et al., 2010). This correction assumes that the positive artifact is similar throughout the United States and also assumes that organic vapors are adsorbed uniformly throughout the front and back filters. These assumptions may not always be appropriate (Watson et al., 2009). Typical artifacts for OC can correspond to half of the reported ambient concentration (McDade et al., 2004). Negative artifacts due to the volatilization of particulate organics are not accounted for because they are thought to be small (Turpin et al., 2000), although some studies suggest they could be important. Changes in analytical methods due to hardware upgrades on January 1, 2005, resulted in changes in the split between OC and LAC (Chow et al., 2007; White, 2007)). Higher LAC/total carbon ratios were reported after the change in analytical methods, but no changes in total carbon were detected (see Section 1.3.1.1).

Finally, module D is fitted with a PM_{10} inlet and utilizes a Teflon filter. PM_{10} aerosol mass concentrations are determined gravimetrically.

All IMPROVE data are available for download from http://views.cira.colostate.edu/fed/.

1.2.3 Optical Sampling and Analysis

Routine optical monitoring includes light extinction and scattering coefficients as measured by transmissometer and nephelometer, respectively. Optical monitoring is conducted at a subset of IMPROVE monitoring sites. The number of sites has decreased significantly due to budgetary constraints.

The Optec LPV-2 transmissometer (Optec, Inc., Lowell, Michigan) has been used in the IMPROVE network since 1986. The Optec LPV-2 operates at a wavelength of 550 nm over path lengths up to 15 km. Its use in remote locations such as national parks is discussed by Molenar et al. (1989), while its use in urban settings is presented by Dietrich et al. (1989). Data processing

algorithms that incorporate corrections for interferences are thoroughly discussed by Molenar and Malm (1992).

Molenar et al. (1989) discuss the inherent uncertainties associated with the measurement. The accuracy of the transmission measurement, as determined by field and laboratory calibrations, is better than 1%. However, the accuracy of the derived extinction coefficient is dependent on the accuracy of the transmission measurement in field conditions. The transmission calculation is determined from an absolute (as opposed to relative) measurement of irradiance of a light source of known intensity that is located some known distance from the receiver. The measurement is made using optics exposed to the ambient atmosphere but is assumed to be free of dust or other films. The uncertainties associated with these parameters contribute to the overall uncertainty of the measurement. The estimated uncertainty is about 4 Mm^{-1} for a typical 5-km path length. A list of operating and discontinued transmissometers is provided in Table 1.4, including the locations of the receiver and transmitter. Only two transmissometers are currently operating (Bridger, Wyoming, BRID1, and San Gorgonio, California, SAGO1).

Table 1.4. Transmissometer receiver and transmitter locations.

Location	Site Name	Receiver Lon (deg)	Lat (deg)	Elevation (m)	Bearing (deg)	Transmitter Lon (deg)	Lat (deg)	Elevation (m)	Mean Elevation	Elevation Angle (deg)	Distance	Start Date	End Date	Sponsor
ACAD1	Acadia NP	-68.26	44.37	122	134	-68.23	44.35	466	300	5	4	11/12/1987	6/9/1993	NPS
BADL1	Badlands NP	-101.9	43.79	772	239	-101.95	43.77	805	805	-0.01	4.151	1/13/1988	9/30/2006	NPS
BAND1	Bandelier NM	-106.26	35.78	2028	315	-106.3	35.81	2143	2077	1.65	4.058	10/5/1988	9/30/2006	NPS
BIBE2	Big Bend NP	-103.21	29.39	1037								1/27/2000	10/1/2005	NPS
BIBE1	Big Bend NP	103.21	29.35	1082								12/1/1988	8/28/2003	NPS
BRID1	Bridger WA	-109.79	42.93	2396	11	-109.77	42.97	2568	2479	2.01	5.083	7/20/1988		USFS
CANY1	Canyonlands NP	-109.82	38.46	1809	73	-109.75	38.48	1774	1790	-0.29	6.426	12/20/1986	9/30/2006	NPS
CHIR3	Chiricahua NM	-109.36	32.01	1698								7/1/2001	12/16/2003	NPS
CHIR2	Chiricahua NM	-109.39	32.01	1573	97	-112.54	32.01	1682	1625	2.07	3.18	1/23/1999	7/1/2001	NPS
CHIR1	Chiricahua NM	-109.39	32.01	1567	84	-109.32	32.01	2235	1901	6.26	6.123	2/17/1989	1/1/1999	NPS
CRLA1	Crater Lake NP	-122.05	42.96	2050								9/1/1988	9/10/1991	NPS
GLAC1	Glacier NP	-113.94	48.56	968	232	-113.99	48.53	975	972	0.08	5.276	2/2/1988	9/30/2006	NPS
GRBA1	Great Basin NP	-114.21	38.99	2139	315	-114.24	39.02	2365	2248	3.44	3.913	8/20/1992	9/30/2006	NPS
GRCA1	Grand Canyon NP	-111.99	36.0	2256	81	-111.93	36.01	2170	2213	-0.85		12/18/1986	10/1/2007	NPS
	Grandview (on the rim)													
GRCW1	Grand Canyon NP	-112.12	36.07	2177	205	-112.09	36.11	755	1450	-15.78	5.11	12/13/1989	10/1/2007	NPS
	Yavapai (in canyon)													
GUMO1	Guadalupe Mountains NP	-104.81	31.83	1664	249	-104.86	31.82	1317	1467	-3.53	4.858	11/17/1988	9/30/2006	NPS
MEVE2	Mesa Verde NP	-108.49	37.22	2245								7/19/1991	7/28/1993	NPS
MEVE1	Mesa Verde NP	-108.49	37.20	2205								9/15/1988	7/23/1990	NPS
PEFO1	Petrified Forest NP	-109.77	35.08	1755	173	-109.75	34.94	1690	1731	-0.3	15.44	4/17/1987	7/6/1987	NPS
PEFO2	Petrified Forest NP	-109.8	34.9	1698	48	-109.75	34.95	1700	1695	0.1	5.938	7/1/1987	11/30/2004	NPS

Location	Site Name	Receiver Lon (deg)	Lat (deg)	Elevation (m)	Bearing (deg)	Transmitter Lon (deg)	Lat (deg)	Elevation (m)	Mean Elevation	Elevation Angle (deg)	Distance	Start Date	End Date	Sponsor
PINN1	Pinnacles NM	-121.15	36.47	448	317	-121.18	36.5	428	438	-0.25	4.799	3/23/1988	7/25/1993	NPS
ROMO1	Rocky Mountain NP	-105.58	40.36	2536	305	-105.63	40.39	2932	2734	4.31	5.274	11/25/1987	7/8/1997	NPS
ROMO2	Rocky Mountain NP	-105.58	40.37	2413	302	-105.63	40.39	2932	2717	5.01	4.921	10/3/1998	9/30/2006	NPS
SAGO1	San Gorgonio WA	-116.91	34.19	1679	211	-116.94	34.16	1731	1721	0.29	4.099	4/27/1988	5/31/2006	USFS
SAGO1	San Gorgonio WA	-116.91	34.19									3/8/2007		USFS
SHEN2	Shenandoah NP	-78.42	38.51	1054	310	-78.44	38.52	1061	1717	-0.49	1.412	9/15/1991	10/30/2003	NPS
SHEN1	Shenandoah NP	-78.43	38.51	1061								12/8/1988	3/22/1991	NPS
TONT1	Tonto NM	-111.03	33.62	733	115	-111.11	33.65	786	760	0.42	7.203	4/12/1989	9/17/1991	NPS
YELL1	Yellowstone NP	-110.69	44.97	1836	125	-110.65	44.95	1951	1894	1.54	4.285	7/18/1989	7/28/1993	NPS
YOSE1	Yosemite NP	-119.7	37.71	1608	242	-119.73	37.7	1370	1489	-5.04	2.711	8/18/1988	9/30/2006	NPS

NM = National Monument
NP = National Park
WA = Wilderness Area

The Optec NGN-2 open air nephelometer measures total ambient light scattering coefficients for all particles sizes at an effective wavelength of 550 nm (Molenar, 1989). The instrument's open-air design has minimal heating and allows a larger distribution of particle sizes to pass through it. It is also designed with solid-state electronics that are very stable over a wide temperature and humidity range. It still has an inherent limitation of an abbreviated acceptance angle in that it only samples light scattered between 5° and 175°, and the cut point of the instrument has not been characterized. Calibration of the instrument and data validation and processing algorithms are discussed in detail in Molenar and Malm (1992). Unlike transmissometers, where an uncertainty in transmittance leads to an additive error in extinction coefficients, uncertainties in nephelometer calibration lead to multiplicative errors in measured scattering coefficients. Typical uncertainties for the Optec NGN-2 are on the order of 5–10% (Molenar and Malm, 1992).

During high humidity and precipitation events, the nephelometer can report erroneously high scattering coefficient values. This is due to water condensing on the walls of the nephelometer and spray from rain drops impacting the screen on the nephelometer inlet. This water collects in the light trap and reflects light directly into the scattered-light detector, causing extremely high readings. In order to minimize this problem, the door of the nephelometer closes during heavy precipitation events, and a wick was added to the light trap to facilitate the removal of any collected water. A list with nephelometer sites is provided in Table 1.5. Sixteen nephelometers are currently in operation.

Table 1.5. IMPROVE nephelometer network site locations.

Site	Code	State	Latitude	Longitude	Elevation	Start Date	End Date
Acadia NP	ACAD1	ME	44.37	-68.26	122	6/10/1993	12/1/1997
Acadia NP	ACAD2	ME	44.38	-68.26	158	12/1/1997	
Big Bend NP	BIBE1	TX	29.30	-103.18	1052	2/1/1998	
Desolation WA	BLIS1	CA	38.98	-120.11	2109	8/12/1996	6/1/2006
Boundary Waters Canoe Area WA	BOWA1	MN	47.95	-91.50	515	5/4/1993	9/30/1997
Cedar Bluff State Park	CEBL1	KS	38.70	-99.76	669	9/1/2004	8/31/2007
Chiricahua National Monument	CHIR1	AZ	32.01	-109.39	1570	12/1/2003	9/30/2007
Chiricahua National Monument	CHIR1	AZ	32.01	-109.39	1570	10/1/2007	5/11/2010
Tucson	CHPA1	AZ	32.30	-110.98	704	6/1/2003	10/1/2010
Columbia River Gorge National Scenic Area	COGO2	WA	45.57	-122.21	240	6/1/2001	3/9/2005
Cohutta WA	COHU1	GA	34.79	-84.63	743	2/1/2004	3/31/2007
Columbia River Gorge National Scenic Area	CORI1	WA	45.66	-121.00	198	8/25/1993	5/1/2000
Columbia River Gorge National Scenic Area	CORI1	WA	45.66	-121.00	198	6/1/2001	3/9/2005
Tucson	CRAY1	AZ	32.20	-110.88	809	2/1/2001	10/1/2010
Dolly Sods WA	DOSO1	WV	39.11	-79.43	1158	5/9/1993	9/30/1997
Dolly Sods WA	DOSO1	WV	39.11	-79.43	1158	11/1/2003	11/30/2006
Phoenix	DYRT1	AZ	33.64	-112.34	364	7/1/2003	
Edwin B. Forsythe NWR	EBFO1	NJ	39.47	-74.45	5	4/14/1993	4/1/1994
Phoenix	ESTR1	AZ	33.39	-112.39	290	2/1/2003	
Gila WA	GICL1	NM	33.22	-108.23	1783	4/1/1994	10/1/2003
Glacier NP	GLAC2	MT	48.51	-114.00	939	11/7/2007	

Site	Code	State	Latitude	Longitude	Elevation	Start Date	End Date
Great Basin NP	GRBA2	NV	39.01	-114.22	2052	1/23/2008	
Mount Baldy WA	GRER1	AZ	34.06	-109.44	2513	5/1/2001	5/11/2010
Great Gulf WA	GRGU1	NH	44.31	-71.22	439	6/7/1995	3/31/2005
Great Smoky Mountains NP	GRSM1	TN	35.63	-83.94	793	4/28/1993	
Green River Basin	GRVS1	WY	41.84	-109.61	1951	7/1/1996	10/17/2000
Grand Canyon NP	HANC1	AZ	35.97	-111.98	2235	12/18/1997	
Pine Mountain WA	HUMB1	AZ	33.98	-111.80	1586	3/1/1997	11/1/2003
Mazatzal WA	IKBA1	AZ	34.34	-111.68	1280	6/1/2001	5/11/2010
Grand Canyon NP	INGA1	AZ	36.08	-112.13	1164	6/1/2004	
Jarbidge WA	JARB1	NV	41.89	-115.43	1889	4/9/1993	9/30/1997
James River Face WA	JARI1	VA	37.63	-79.51	299	12/5/2000	10/1/2003
Lone Peak WA	LOPE1	UT	40.45	-111.70	1740	11/16/1993	9/1/2001
South Lake Tahoe	LTBV1	CA	38.95	-119.96	1902	2/1/1996	5/1/2004
South Lake Tahoe	LTBV2	CA	38.93	-119.96	1904	12/1/2005	6/30/2006
Lye Brook WA	LYBR1	VT	43.15	-73.12	1010	8/5/1993	3/31/1994
Lye Brook WA	LYBR1	VT	43.15	-73.12	1010	5/30/1996	12/31/2000
Lye Brook WA	LYBR1	VT	43.15	-73.12	1010	1/1/2001	10/1/2003
Mammoth Cave NP	MACA1	KY	37.22	-86.07	219	3/11/1993	7/1/1997
Mammoth Cave NP	MACA2	KY	37.13	-86.15	243	7/23/1997	
Mayville	MAYV1	WI	43.44	-88.53	306	11/1/2000	12/31/2006
Mazatzal WA	MAZA1	AZ	33.91	-111.41	2164	4/1/1997	8/30/2000
Sierra Ancha WA	MCFD1	AZ	33.91	-110.97	2175	10/30/1997	2/1/2000
Milwaukee	MILW1	WI	43.00	-87.89	193	6/1/2004	6/30/2006
Mount Rainier NP	MORA1	WA	46.76	-122.12	423	2/13/1993	
Mount Zirkel WA	MOZI1	CO	40.46	-106.74	3215	11/1/1993	8/1/1994
Mount Zirkel WA	MOZI2	CO	40.54	-106.68	3242	11/5/1993	7/31/2009
Galiuro WA	MUSR1	AZ	32.33	-110.23	1402	7/8/1997	6/30/2005
National Capitol - Central	NACA1	DC	38.88	-77.03	20	4/24/2003	
Nebraska National Forest	NEBR1	NE	41.89	-100.34	888	8/10/2005	8/31/2007
Okefenokee NWR	OKEF1	GA	30.74	-82.12	15	2/12/1993	6/24/1997
Organ Pipe Cactus National Monument	ORPI1	AZ	31.95	-112.80	514	6/1/2003	5/11/2010
Petrified Forest NP	PEFO3	AZ	34.82	-109.89	1709	11/18/2003	9/30/2007
Petrified Forest NP	PEFO3	AZ	34.82	-109.89	1709	10/1/2007	5/11/2010
Phoenix	PHON1	AZ	33.50	-112.10	366	4/1/1997	9/30/2009
Quaker City	QUAK1	OH	39.94	-81.34	372	3/26/2002	1/14/2004
Superstition WA	QUVA1	AZ	33.29	-111.29	668	6/1/2003	5/11/2010
Cape Romain NWR	ROMA1	SC	32.94	-79.66	2	1/1/2004	
Rocky Mountain NP	ROMO3	CO	40.28	-105.55	2735	12/31/2007	
Chiricahua WA	RUCA1	AZ	31.78	-109.30	1637	11/17/1997	5/1/2001
Seney NWR	SENY1	MI	46.29	-85.95	227	1/7/2002	7/1/2006
Shenandoah NP	SHEN1	VA	38.52	-78.43	1073	9/19/1996	
Shining Rock WA	SHRO1	NC	35.38	-82.77	1612	6/8/1994	8/1/1999
Sierra Ancha WA	SIAN1	AZ	34.09	-110.94	1595	8/1/2000	5/11/2010
Alpine Lakes WA	SNPA1	WA	47.42	-121.43	1152	8/26/1993	5/1/2001
Sycamore Canyon WA	SYCA1	AZ	35.14	-111.97	2040	7/1/1998	5/11/2010
Three Sisters WA	THSI1	OR	44.29	-122.04	881	7/23/1993	5/1/2001
Tucson	TUCN1	AZ	32.24	-110.96	745	4/1/1997	4/8/2009
Saguaro NP	TUMO1	AZ	32.28	-111.17	754	12/1/1996	11/1/2001
Saguaro NP	TUMO2	AZ	32.25	-111.22	718	11/1/2001	5/11/2010
Upper Buffalo WA	UPBU1	AR	35.83	-93.20	701	2/26/1993	9/30/1997
Upper Buffalo WA	UPBU1	AR	35.83	-93.20	701	9/1/2004	10/1/2009
Phoenix	VEIX1	AZ	33.46	-112.00	345	6/1/2003	

Site	Code	State	Latitude	Longitude	Elevation	Start Date	End Date
Virgin Islands NP	VIIS1	VI	18.34	-64.80	64	4/23/1998	9/30/2005
Wichita Mountains NWR	WIMO1	OK	34.73	-98.71	517	9/1/2004	8/31/2007

NP = National Park
NWR = National Wildlife Refuge
SP = State Park
WA = Wilderness Area

1.3 PROTOCOL AND EQUIPMENT CHANGES

While consistency through time is critical to a monitoring program interested in trends, changes in sampling, analysis, and data-handling protocols and equipment are inevitable in any long-term monitoring program. Significant changes in sampling, analysis, and data processing have occurred in the history of the IMPROVE network. Most of the changes were implemented to improve the quality or usefulness of the IMPROVE dataset or to increase the overall effectiveness of the network within available resources. Assessments were conducted prior to many of the changes to assess and, where possible, identify approaches that would minimize the effects of changes on the dataset. In addition, IMPROVE routinely conducts data consistency assessments, specifically designed to identify and attempt to explain data discontinuities and trends that are not thought to be associated with changes in atmospheric conditions. The results of these assessments are used to inform decisions concerning the operation of IMPROVE and to alert data users via data advisories posted on the IMPROVE website.

This section encompasses changes that have occurred since the last IMPROVE report was published in 2006 (Debell, 2006), covering samples collected from January 2005 to the present. Some of the key changes, including the reasoning behind the decision and the ramifications for the IMPROVE dataset, are described below and listed in Table 1.7. The final subsection describes some inadvertent changes or interferences that were discovered in the course of data analysis and quality control review. Many of the summaries in this section are referenced to data advisories on the IMPROVE website that provide additional information, including data plots and useful graphics.

1.3.1 Analytical Changes

1.3.1.1 Introduction of a New Model Carbon Analyzer

Organic carbon (OC) and light absorbing carbon (LAC) on quartz filters have been quantified by the Desert Research Institute (DRI) since the beginning of the IMPROVE network, using laboratory analyzers developed at the Oregon Graduate Center (OGC). These instruments use a thermal/optical reflectance (TOR) protocol to determine OC and LAC.

By the late 1990s it was evident that the DRI/OGC analyzers were deteriorating. Some components were no longer manufactured and the data acquisition system was antiquated. The Model 2001 (Atmoslytic Inc., Calabasas, CA) analyzer was developed and made commercially available as a replacement. The Model 2001 has a number of enhancements, including better characterization of sample temperature and sample atmosphere, automatic sample positioning, more rapid temperature response, improved seals and flow control, greater heating capacity, advanced electronics, modern data acquisition, the potential for an automated sample changer,

and the ability to simultaneously measure reflectance and transmittance. Concurrent with the hardware modifications was the application of a new TOR protocol, named IMPROVE_A, designed to reflect the more accurate and less variable temperature and instrument-atmospheric conditions provided by the new instruments.

The Model 2001 analyzer was applied for routine analysis of IMPROVE samples collected on or after January 1, 2005. Extensive testing prior to deployment had suggested that observable differences in the data record would be minimal (Chow et al., 2005). However, subsequent examination of data from the first two years of analysis (2005 and 2006) revealed unforeseen differences between data from the old and new instruments (White, 2007a). The differences vary as a function of site, but the new data generally identify a higher proportion of total carbon as LAC and a lower proportion as OC than were observed in the final years of the old instruments. The LAC/OC distinction is operationally defined, and the differences are not fully understood.

1.3.1.2 Transition from He Flush to Vacuum Chamber Cu-Anode XRF

Light-element concentrations in samples collected after December 1, 2001, have been determined by X-ray fluorescence (XRF) analysis using a Cu-anode tube as the source. Until 2005, analyses were conducted at ambient pressure in a He-flushed atmosphere. That system was replaced on January 1, 2005 (sample date), with a new system that operates under vacuum.

In 2001 proton-induced X-ray emission (PIXE) switched to He-flushed XRF and resulted in substantially decreased sensitivity for sodium, the lightest of the elements reported. Sensitivities improved for 2005 and later samples after the conversion of the XRF system to vacuum operation but are still below those from PIXE (White, 2007b).

A second vacuum XRF system, with the same design, was then developed and tested for equivalence with the first (White, 2007c). Samples collected in October 2005 were the first to be reported from the second system. Data from samples collected after October 1, 2005, are reported with an added indicator of the Cu-anode XRF system used in analysis: the first (1) or the second (2). (All light-element data from January through September 2005 samples are from the first system.)

The two Cu-anode systems are designed to be equivalent and are calibrated against the same reference foils. The two systems report concentrations for the single-element calibration foils that agree within prescribed tolerances. However, the two systems do exhibit some detectable differences for actual samples.

1.3.1.3 Introduction of New Calibration Foils for Mo-Anode XRF

A molybdenum-anode XRF instrument is used to analyze the heavier elements (Ni, Cu, Zn, As, Se, Br, Rb, Sr, Zr, and Pb). During the analysis of September 2005 samples, new calibration foils with lighter deposits were acquired and used in the Mo-anode XRF system (Flocchini, 2007). The new calibration foils resulted in changes to the calibration factors for the elements Ni, As, Se, Br, Rb, and Pb that could be observed in their effects on reported ambient concentrations.

The new foils represent an attempt to utilize reference foils that more closely match ambient samples in loading. These foils were used in preparing a calibration table that provides the reference points for converting the X-rays collected during analysis to elemental concentrations on filter samples collected in the atmosphere. The uncertainties quoted by the manufacturer for these new foils were ±10% compared to ±5% for the older, more heavily loaded foils. After a number of ambient samples had been analyzed, it became apparent that these new foils resulted in ambient concentrations that were inconsistent with those observed in prior years.

Changes in the percent change in the calibration factors with the old standards compared to the new standards ranged from 0% (no change) for Sr and Zr to -76% change for As. The percentages represent the differences between the last calibration performed with the old foils and the first calibration performed with the new foils. The calibration factors are multiplicative factors in the estimations of the reported concentrations that can introduce systematic biases between the previous and current data. The resulting shifts in concentration must be accounted for in any analysis of trends.

1.3.1.4 Processing XRF Calibration Data

XRF sulfur data reported for sample dates in 2004 and most of 2003 were based on a nonstandard value for the sulfur calibration foil: the value 12.0 µg cm^{-2} was substituted for the value 13.8 µg cm^{-2} quoted by the supplier (White, 2006a). The adjusted value was used as early as February 2003 and may have been used still earlier. The rationale for using an adjusted value was not documented and may have been to improve agreement with ion-chromatographic sulfate measurements.

Sulfur data for sample dates beginning in January 2005 are based on the quoted value of the foil, which yields higher reported values by the factor 13.8/12.0 = 1.15, or 15%. This reporting change, not the simultaneous switch from a helium-flushed system to one operating in vacuum, accounts for the bulk of the increase in reported sulfur relative to reported $SO_4^{=}$ between December 2004 and January 2005. The magnitude of the reporting change is small relative to the range of sulfur concentrations reported across the network. However its systematic impact is likely to be evident in interannual comparisons and should be accounted for in their interpretation.

The procedure for analyzing XRF system calibration data was modified beginning with samples collected in January 2007. In prior years the calibration for any element had been based upon the quoted concentration of the calibration standard foil for that element, as reported by Micromatter, the manufacturer of the standard foils. Beginning with the January 2007 data, a standard was analyzed for each element and then a smooth curve was drawn through the resulting instrument responses. The curve fit value for each element was then used as the basis for calibration. This new curve fitting approach was initiated in an attempt to dampen the concentration uncertainty associated with any single standard foil. The result is a shift in the typical concentrations reported for some elements.

1.3.1.5 New XRF Quality Assurance Reports & Clarification of Data Acceptance Criteria

Beginning with samples collected in January 2005, quarterly reports have been prepared to summarize the findings of quality control checks on the XRF data (http://vista.cira.colostate.edu/improve/Data/QA_QC/QAQC_UCD.htm). January 2005 also marked the initial use of the vacuum chamber Cu-anode XRF system, which replaced the helium flush system.

The quarterly reports present detection rates for each element, as well as results from calibrations and calibration checks, X-ray energy calibrations, field blank analyses, reanalysis of selected filters, and comparison of the Cu and Mo anode systems for elements measured on both. The reports also document the system settings that were used for that quarter's analytical session.

The initiation of quarterly reports in 2005 also marked the formalization of acceptance criteria for XRF data. The performance of the systems is monitored approximately weekly by monitoring the ratios of the system response at each calibration check to the response observed at the last calibration. If the ratios lie within the acceptance limits 0.9–1.1 for all quantitative elements, then the system is considered stable and the existing calibration factors continue to be used. Deviations beyond 10% trigger an investigation of the problem and possible system recalibration. After a recalibration, all samples analyzed since the last successful calibration verification are reanalyzed with the new calibration factors.

1.3.2 Sampling Equipment Changes

1.3.2.1 Filter Masks Removed

Until recently, masks were used at many sites to reduce the nominal collection area of module A filters from 3.53 cm^2 to 2.20 cm^2. Masking improved XRF sensitivities at low concentrations, but caused occasional clogs at high concentrations. By the beginning of 2008, all filters had been unmasked.

A relative bias between masked and unmasked elemental measurements can be seen by comparing the sulfur/sulfate ratios measured under both conditions, as sulfate ion concentrations have been measured by the same protocol at all sites since 2001 (White, 2008). Unmasked sites have generally reported about 5% more sulfur than masked sites at a given measured sulfate concentration, and the sulfur reported from masked sites has typically risen by about 5% when they have converted to unmasked operation. It is not known whether these differences reflect under-reporting from masked samples, over-reporting from unmasked samples, or contributions from both.

IMPROVE's hybrid integrating plate/sphere (HIPS) is designed to measure the absorption thickness of a Teflon filter sample. Absorption thickness can be thought of as the absorption cross-section ($m^2\ g^{-1}$) of the absorbing material times the material's areal mass loading ($g\ m^{-2}$) on the filter. Well-recognized artifacts of the method cause measured absorption to increase less than proportionately with the mass loading. Because masking generates higher areal loadings at the same atmospheric concentrations, some bias toward lower absorption

readings for masked samples can be expected to result from this loading dependence (White, 2010).

1.3.2.2 Quartz Backup Filters Added at Six Sites

For many years the IMPROVE network has collected quartz backup filters behind the primary quartz filters at six sites. IMPROVE has used the monthly median carbon data from these six sites to adjust for a presumed positive artifact for all sites in the network. Experts from IMPROVE and other similar networks met at a carbon particulate matter monitoring workshop in January 2008 to consider improvements to this approach for estimating sampling artifacts. Their focus was on improving spatial coverage, understanding urban/rural differences, and better understanding the observed relationship between front filter and backup filter organic carbon concentrations The following recommendations were phased into the IMPROVE network between mid-2008 and mid-2009:

- Continue quartz backup filters at the six original sites: Chiricahua, Arizona (CHIR1), Grand Canyon (GRCA2), Mount Rainier, Washington (MORA1), Okefenokee, Georgia (OKEF1), Shenandoah, Virginia (SHEN1), and Yosemite (YOSE1). Inaugurate backup filters at six additional sites: Blue Mounds, Minnesota (BLMO1), Hercules-Glades, Missouri (HEGL1) (both collocated samplers), Lye Brook, Vermont (LYBR1), Phoenix (PHOE1) (both collocated samplers), Washington, D.C. (WASH1), and Yellowstone (YELL1).
- Collect quartz field blanks only at the sites listed above and discontinue them elsewhere in the network. Collect a set of field blanks with every filter cartridge (every week, beginning on Tuesday). To conserve funding, only two-thirds of the field blank sets will be analyzed, only those for weeks beginning or ending with a Tuesday sampling day. Both the front and back field blanks will be analyzed. The field blanks from the intervening week will be archived but will not be analyzed.
- Only backup filters collected during the weeks of field blank analysis will be analyzed, i.e., two-thirds of the secondary filters. The backup filters from the intervening week will be archived but will not be analyzed. All sampled front filters will be analyzed, from all weeks.

1.3.2.3 New Cassette Design for the IMPROVE Sampler

The IMPROVE group at UC Davis has developed a new filter cassette design that will be implemented in the IMPROVE network during 2011. In the new design the metal screen that supports the filter is detached, unlike the older screens which were permanently attached to the plastic cassette body. This new design results in more consistently uniform sample deposits on the filters, thereby improving the reliability of measurements such as the XRF analysis that is used to determine elemental concentrations.

The new cassette design is shown in Figure 1.5. The metal screen can be removed by the technicians for cleaning and then re-installed along with a clean filter for the next sampling event. Once the cassette is reassembled with the cassette cap in place, the filter fits snugly against the screen, just as it did with the old design. For comparison, Figure 1.6 shows the old cassette design, with the screen permanently attached. Because the cassettes are serviced and

reassembled in the UC Davis laboratory, the change to the new cassette screens is transparent to the site operators. The assembled cartridges that are shipped to the sites in blue shipping boxes look the same before and after the change to the new screens.

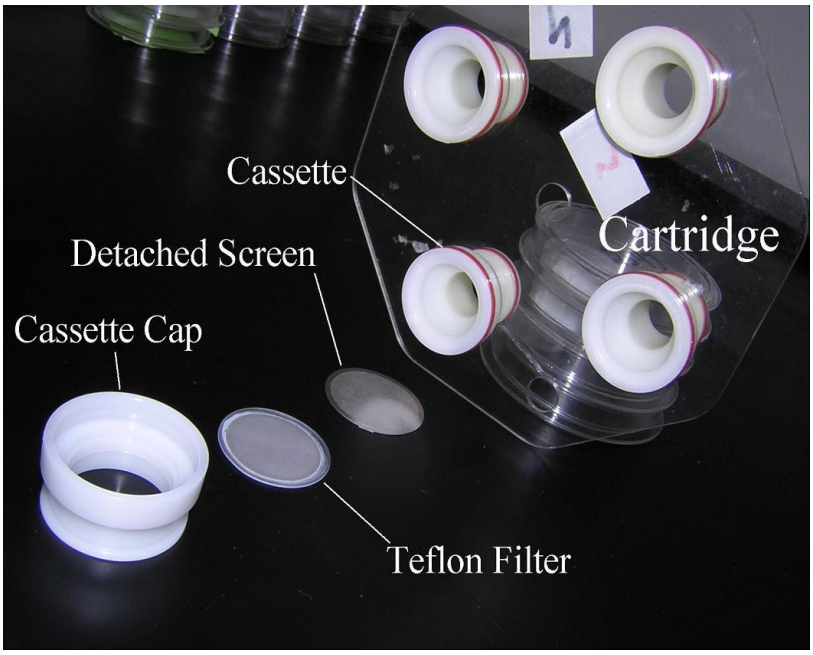

Figure 1.5. Detached screen cassette.

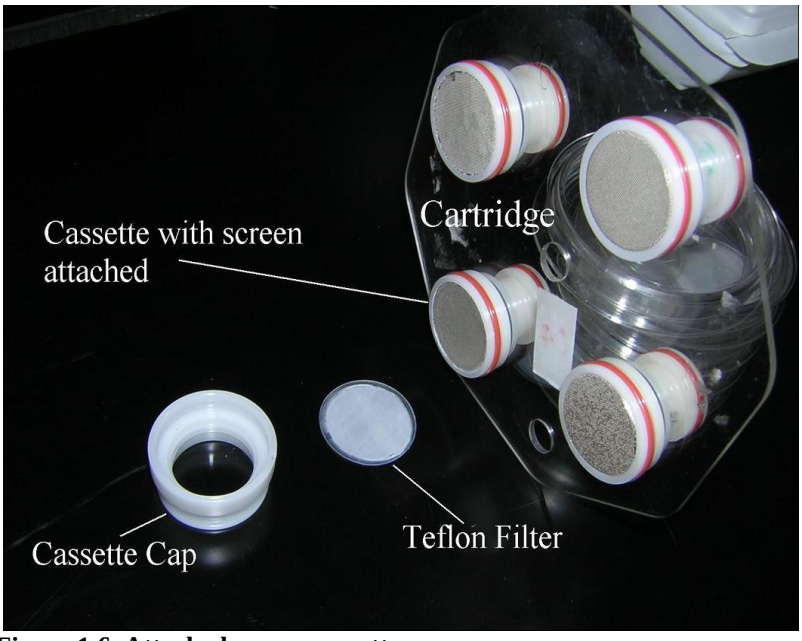

Figure 1.6. Attached screen cassette.

The switch to the new design was motivated initially by some changes in the cassette manufacturing process. The IMPROVE network was in need of additional cassettes to replace damaged pieces and to accommodate new sites. Due to some engineering changes in the manufacturer's shop it was no longer possible to manufacture cassettes in precisely the same configuration as the existing cassettes. Attempts were made to produce a modified attached

screen cassette that would be comparable to those already in use in the network. However, field tests of attached screen prototypes using the manufacturer's modified approach were unable to demonstrate satisfactory measurement agreement with the existing design.

Reengineering of the cassette design was needed to achieve comparability between the old and new units, so the UC Davis group decided to take advantage of the opportunity to come up with a superior design. Their literature review found that essentially all samplers used in other aerosol networks employ a detached screen design. Furthermore, initial prototype tests indicated that a detached screen design would improve sample uniformity. A redesign and testing program led to the final detached screen cassette design to be deployed in the network.

Prototype units of the new detached screen design were prepared and tested extensively at UC Davis to ensure comparability with the existing attached screen design. UC Davis has an outdoor IMPROVE sampler test facility where up to sixteen sampler modules can be operated concurrently. Tests were run using paired sets of attached and detached screen cassettes, all sampling the ambient UC Davis air at the same time. The flow rate through each sampler module was carefully set and calibrated so that flow rate differences among the modules would be insignificant, thereby ensuring that the flow rate-dependent cyclone particle size cutpoint would be the same for each module.

Teflon filter samples were collected at UC Davis and then were weighed and subjected to XRF analysis to determine elemental concentrations and to laser absorption measurements to quantify aerosol light absorption. These tests demonstrated that samples collected using the old attached screen cassettes and the new detached screen cassettes were comparable. The differences observed between the sets were very small and were well within the statistical uncertainty of the routine IMPROVE measurements.

Because multiple samples from each cassette type were acquired during each test, it was also possible to determine the measurement precision within each type. These results indicated that the precision of the mass and elemental measurements using the new detached screen design is typically tighter, a welcome improvement over the existing design.

The improved precision is likely the result of improved sample uniformity. Figures 1.7 and Figure 1.8 show typical sample deposit patterns using attached and detached screens, respectively. The deposit on the attached screen filter exhibits non-uniformity around the edge of the filter. The edge areas with no deposit are a result of the process used to press the screen into the plastic cassette body, whereby plastic clogs some of the screen holes around the perimeter. The deposit on the detached screen filter exhibits no edge effects, since intact holes extend all the way to the edge of the filter.

Figure 1.7. Filter sample collected using attached screen cassette.

Figure 1.8. Filter sample collected using detached screen cassette.

New screens are being purchased for all cassettes, but the existing plastic cassette bodies can be used with the detached screen design. Equipment in the UC Davis machine shop is used to punch the attached screen out of each unit and then smooth any rough edges that remain on the plastic body. Once that quick procedure is completed the detached screen fits precisely into each cassette body. Some new cassette bodies, identical to the existing ones, have also been purchased to increase the inventory of available cassettes.

Only the 25 millimeter cassettes are being converted to the detached screen design. The 37 millimeter B-module cassettes will remain unchanged and will retain the attached screen design. The 37 millimeter nylon filters are extracted in solution which is then used for ion analysis, so the uniformity of the sample deposit does not influence the analysis.

The 25 millimeter cassettes used in the A, C, and D modules are all being converted to the detached screen design in order to achieve consistency throughout the measurement set. However, the benefits of improved sample uniformity are expected only for the A-module Teflon® filter. XRF, laser absorption, and proton beam hydrogen measurements apply an incident beam that covers only the central portion of the filter, so uniformity is crucial in extrapolating the results to the entire filter. The D-module PM_{10} Teflon filters are weighed only, so sample uniformity does not impact the analysis.

The C-module employs a quartz filter, with physical characteristics that differ from Teflon. Teflon is a plastic and Teflon filters are pulled down firmly to the surface of the screen when the vacuum pump is on. Hence, sample material is deposited only in the immediate area of the screen holes, so the characteristics of the screen can influence the sample deposit. The "imprint" of the screen holes can be seen clearly when Teflon filter deposits are viewed under a microscope. Quartz filters, on the other hand, are made of multiple layers of randomly oriented media and have a porous or fibrous texture that distributes the sample uniformly across the entire filter surface, independent of the geometry of the backing screen.

1.3.3 Data Processing Changes

1.3.3.1 Change in the Definition of Flow Rate Native Flags

Recent work performed to characterize the IMPROVE cyclone suggested that the equations relating cut point to flow rate developed at UC Davis are invalid (J. Turner, 2006, personal communication). Therefore, the native validation flags based on flow rate have been revised and applied to samples collected in January 2005 and onward (McDade, 2007).

The IMPROVE cyclone is based on the AIHL cyclone specifications. The recent characterization work was consistent with the original AIHL characterization performed by John and Reischl (1980), and it was therefore decided to use the original John and Reischl (1980) equation for the IMPROVE cyclones used in the A, B, and C sampler modules (J. Turner, 2006, personal communication). The John and Reischl (1980) equation is much less sensitive to flow rate than the UC Davis equation used in the past, and the cut point is 2.4 μm rather than 2.5 μm at the IMPROVE nominal flow rate of 22.8 LPM.

UC Davis applies one of four "native" (i.e., initial) flags to data to indicate unusual flow rates: CL (clogged), CG (clogging), RF (extremely high or low flow rate), and LF (moderately high or low flow rate). The CL flag is based on the accuracy of the flow rate equation and is therefore not affected by this new cyclone information. The criteria for CG and RF flow rate flags are now stricter in terms of cut point because the cut point equation is less sensitive to flow rate. These criteria apply only to modules A, B, and C. The numerical flow rate criterion for the LF flag has been altered because the prior criterion is not centered on 2.5 μm as a result of the shift in the equation. The native flags LF and RF translate to a V5 status flag in the IMPROVE

VIEWS database, native flag CG translates to a V6 status flag, and native flag CL translates to an M3 status flag. Table 1.6 provides the validation flags and how they have been applied.

Table 1.6. Updated flow rate-related validation flag definitions and application criteria.

Validation Flag	Definition	Concentration Reported?	Old Criteria: applied to Jan 2000 through Dec 2004 samples	Updated criteria: applied to samples collected in Jan 2005 and onward
CL	Clogged filter	No	Flow rate less than 15 LPM for more than 1 hour	Same criterion: based on the flow rate calculation inaccuracy not cut point
CG	Clogging filter	Yes	Flow rate less than 18 LPM for more than 1 hour	Same criterion: corresponds to a cut point of 3 μm
LF	Low/high flow rate	Yes	Average flow rate results in cut point outside 2 to 3 μm (corresponds to flow rates of 21.3 LPM and 24.3 LPM).	Average flow rate results in cut point outside 2.25 to 2.75 μm : corresponds to flow rates of 19.7 and 24.1 LPM
RF	Really high flow rate	Yes	Average flow rate greater than 27 LPM	Same criterion: corresponds to a cut point of 2 μm

1.3.4 Changes or Interferences Noted Through Data Analysis

1.3.4.1 Sulfur Interference in the Determination of Silicon

The primary XRF peak for sulfur has a shoulder that overlaps the primary XRF peak for silicon. Due to this peak interference, accurate determination of Si is difficult when S concentrations greatly exceed Si concentrations (White, 2006b). Reported concentrations then depart from expectations based on Fe and other crustal elements.

The degree of interference by S is sensitive to details of system performance that can change from month to month. Furthermore, reported uncertainties and detection limits for Si do not adequately account for the interference by S. Data analysts are encouraged to distrust reported Si concentrations when [S] >> [Si] and to disregard reported uncertainties and MDLs for Si.

1.3.4.2 Shifts in the $S/SO_4^=$ Ratio

Most fine-particle sulfur is present as sulfate. Measured concentrations are therefore expected to exhibit a sulfur-to-sulfate mass ratio of approximately 1 to 3. Reported concentrations often depart from this ratio by more than their reported uncertainties (White, 2007d). Empirical evidence points to XRF measurement bias as the source of most of the observed variation. As one example, sulfur/sulfate ratios throughout the network exhibited a decreasing trend during 2003–2004 that was offset by two abrupt increases, each coming at the start of a new sample month. The XRF analyses, unlike the ion-chromatographic analyses, are quality assured in calendar-month batches, and both of the observed jumps coincided with recalibrations of the Cu-anode system used to determine sulfur. The fact that abrupt changes in the sulfur/sulfate ratio were associated with recalibrations of the XRF system suggests that the gradual changes observed at other times may be due to drift in that system's calibration.

A further 15% shift at the start of 2005 was explained as the result of a change in the value used for the sulfur calibration foil from a legacy adjustment to the manufacturer's quote. Since that time further shifts have occurred, including a drop of about 10% in sulfur/sulfate ratios at the start of 2007 (White, 2009). Calibrations in 2005–2006 were based on the quoted value of a foil for each element. Calibrations in 2007–2008 were based on a curve fit to several different elemental foils, and this fit effectively assigned a value to the sulfur foil different from the manufacturer's quote.

The XRF change from helium flushing to vacuum operation at the start of 2005 yielded a somewhat tighter relationship between sulfur and sulfate concentrations. A second vacuum system, designed to be equivalent and calibrated against the same reference foils, was introduced in October 2005 to speed processing. The two systems report concentrations for the single-element foils that agree within prescribed tolerances but exhibit some detectable differences in actual samples. All IMPROVE samples for a given month are analyzed with the same system, and similar intersystem differences for sulfur may contribute some month-to-month variability to the sulfur/sulfate ratio.

Table 1.7. Major networkwide changes in sampling, analysis, and data reporting affecting samples collected January 2005 and later.

Change Date	Change Description
1/1/2005	Changed carbon analysis instrument from DRI/OGC to Model 2001 Thermal/Optical Carbon Analyzer. Changed analysis protocol from IMPROVE to IMPROVE_A
1/1/2005	Changed Cu-anode XRF from helium flush to vacuum chamber system
1/1/2005	Began reporting XRF-determined sulfur based on the quoted value of the calibration foil, replacing empirical value that had been used in 2003 and 2004
1/1/2005	Introduced quarterly XRF QA reports.
1/1/2005	Flow rate native flags revised to reflect new cyclone cut point characterization
9/1/2005	Introduced new calibration foils for Mo-anode XRF system, with lighter deposits
10/1/2005	Introduced a second Cu-anode XRF vacuum chamber system
1/1/2007	Introduced XRF curve fit calibration procedure
12/23/2007	Last sampling date using masked Teflon filters at any site
8/7/2008-6/4/2009	Quartz backup filters added at six sites

1.4. CHEMICAL SPECIATION NETWORK

The objectives of the EPA's Chemical Speciation Network (CSN) are to track progress of emission reduction strategies through the characterization of trends, validation of air quality modeling and source apportionment activities, support of regulatory efforts such as the Regional Haze Rule, and support of health effects and exposure studies. CSN operates approximately 50 long-term trend sites, with another ~150 sites operated by state, local, and tribal agencies, primarily in urban/suburban settings.

The EPA's $PM_{2.5}$ speciation program was established in 1997 as a complement to the $PM_{2.5}$ Federal Reference Method (FRM) mass network. The pilot phase of the program included thirteen sites that operated from February through July 2000. The Speciated Trends Network (now referred to as the CSN) was deployed in the fall of 2000 (U.S. EPA, 2004). Historically, CSN utilized several types of samplers, including the Thermo Andersen RAAS, Met One SASS,

and the URG MASS. The specific sampler employed at a given site was chosen by the state, local, or tribal agency; however, the Met One is the predominant sampler used. All samplers utilize a $PM_{2.5}$ inlet and three channels containing Teflon, nylon, and quartz filters. A magnesium oxide denuder is used ahead of the nylon filter. Samplers operate on a 24-h schedule from midnight to midnight every third day. Supplemental sites may differ in sampler type, analysis laboratory, and sampling schedule (1-in-6 versus 1-in-3 day periods). Filters from most Trend sites are analyzed at the RTI International Laboratory in Research Triangle Park, North Carolina. $PM_{2.5}$ gravimetric mass and elemental compositions are analyzed from the Teflon filter, ions from the nylon filter, and carbon from the quartz filter. The carbon analysis was historically performed using thermal optical transmittance (TOT) using a NIOSH-type protocol. The recognition that IMPROVE samplers and TOR analysis produce different OC and LAC concentrations than CSN samplers and TOT analysis has motivated the CSN transition to TOR analysis for consistency with the IMPROVE network. In addition to the transition from TOT to TOR, in April 2005 the EPA decided to replace the carbon channel sampling and analysis methods with a new, modified IMPROVE version II module C sampler (URG 3000N). The conversion began in May 2007 with 56 sites, followed by another 63 sites in April 2009 and 78 additional sites in October 2009 (U.S. EPA, 2009). Additional detail regarding IMPROVE and CSN sampling and analysis methods for each species is provided in Chapter 2 and includes discussion of aerosol species mass calculations. A discussion of the adjustments applied to CSN carbon data collected prior to the transition to the new analyses and monitors is also included. Adjustments to CSN carbon data were required for IMPROVE and CSN data to be combined. A map of 321 current and discontinued CSN sites is provided in Figure 1.9, with the general regions depicted. We empirically defined 31 regions for the CSN sites based on seasonal distribution of aerosol concentrations and site location. For comparison purposes we grouped sites in regions similar to those defined for the IMPROVE network. Of the 31 regions, eight had only 1 site per region. A list of the 176 sites that met the completeness criteria outlined in Chapter 2 is provided in Table 1.8, including site location, region, and setting (urban, suburban, or rural). The “complete” sites are shown as orange circles on Figure 1.9. CSN data can be downloaded from http://views.cira.colostate.edu/fed/ or http://www.epa.gov/ttn/airs/airsaqs/.

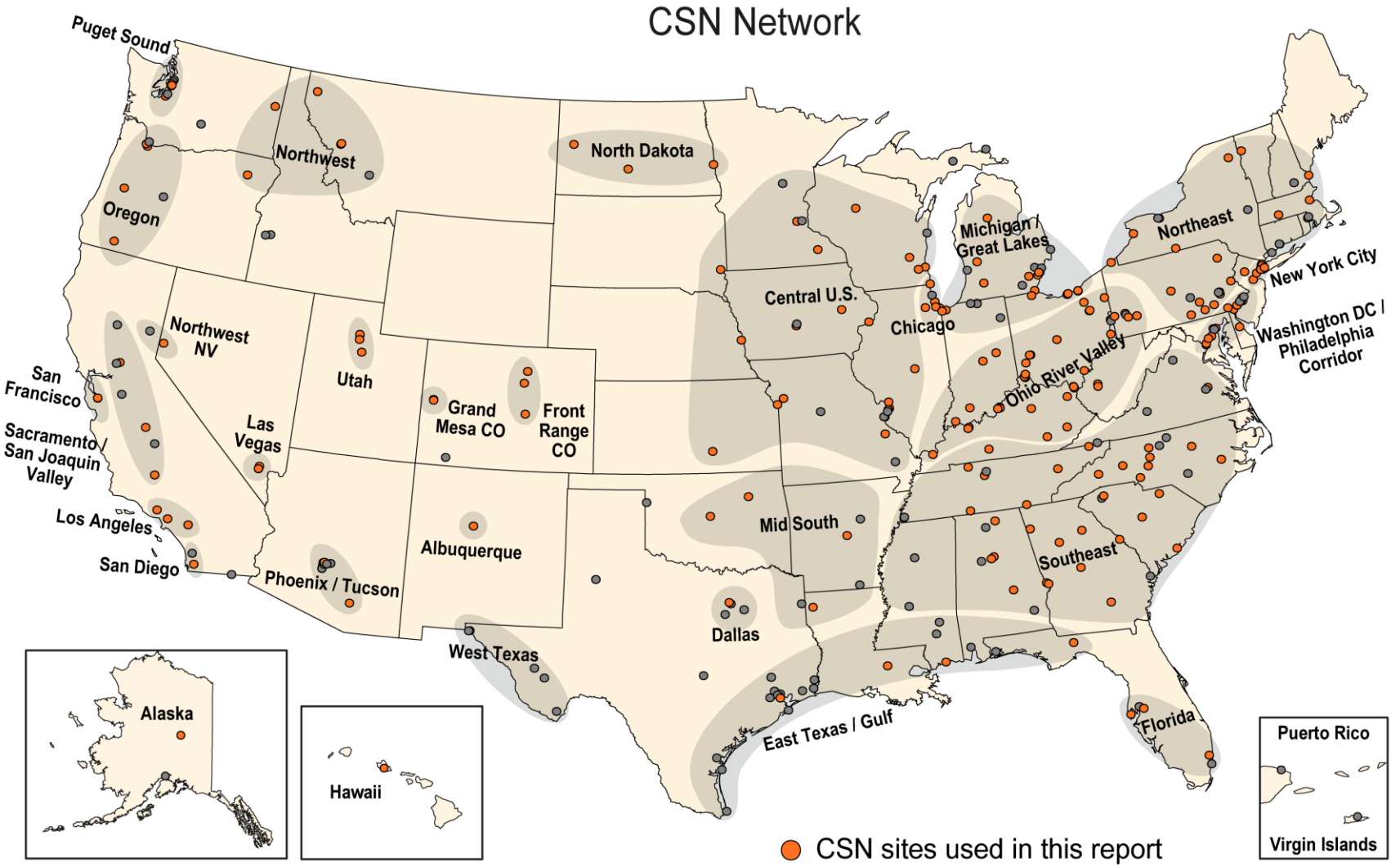

Figure 1.9. Current and discontinued Chemical Speciation Network (CSN) sites (grey and orange) operated by the Environmental Protection Agency. Regions are shown as shaded areas and bold text. The sites included in the analyses in this report are shown as orange circles.

Table 1.8. Chemical Speciation Network (CSN) site location, setting and region.

Site	City	State	Region	Latitude (deg)	Longitude (deg)	Elevation (m)	Setting
10730023	Birmingham	AL	Southeast	33.553	-86.815	177	urban
10732003	Birmingham	AL	Southeast	33.500	-86.924	180	suburban
10890014	Hunstville	AL	Southeast	34.688	-86.586	180	urban
11011002	Montgomery	AL	Southeast	32.407	-86.256	64	suburban
11130001	Phenix City/Columbus	AL	Southeast	32.476	-84.999	91	urban
20900010	Fairbanks	AK	Alaska	64.841	-147.720	132	urban
40139997	Phoenix	AZ	Phoenix/Tucson	33.504	-112.095	355	urban
40191028	Tucson	AZ	Phoenix/Tucson	32.295	-110.982	710	urban
51190007	Little Rock	AR	Mid South	34.756	-92.276	77	urban
60190008	Fresno	CA	Sacramento/San Joaquin Valley	36.781	-119.772	91	suburban
60290014	Bakersfield	CA	Sacramento/San Joaquin Valley	35.356	-119.040	118	urban
60371103	Los Angeles	CA	Los Angeles	34.067	-118.227	126	urban
60658001	Rubidoux	CA	Los Angeles	34.000	-117.416	250	suburban
60670006	Sacramento	CA	Sacramento/San Joaquin Valley	38.614	-121.367	19	suburban
60730003	El Cajon	CA	San Diego	32.791	-116.942	169	suburban
60850005	San Jose	CA	San Francisco	37.349	-121.895	21	urban
61112002	Simi Valley	CA	Los Angeles	34.278	-118.685	308	suburban
80010006	Commerce City	CO	Front Range CO	39.826	-104.937	1558	suburban
80410011	Colorado Springs	CO	Front Range CO	38.831	-104.828	1828	urban
80770017	Grand Junction	CO	Grand Mesa CO	39.064	-108.561	1524	urban
81230008	Platteville	CO	Front Range CO	40.209	-104.823	1464	rural
90090027	New Haven	CT	Northeast	41.301	-72.903	5	urban
100010003	Dover	DE	Washington D.C. /Philadelphia Corridor	39.155	-75.518	6	suburban
100032004	Wilmington	DE	Washington D.C. /Philadelphia Corridor	39.739	-75.558	31	urban
110010043	Washington D.C.	DC	Washington D.C. /Philadelphia Corridor	38.919	-77.013	31	urban
120111002	Davie	FL	Florida	26.083	-80.238	3	suburban
120573002	Valrico	FL	Florida	27.966	-82.230	28	rural
120730012	Tallahassee	FL	East Texas/Gulf	30.440	-84.348	16	suburban
121030026	Pinellas Park	FL	Florida	27.850	-82.715	2	suburban
130210007	Macon	GA	Southeast	32.777	-83.641	103	suburban
130590001	Athens	GA	Southeast	33.946	-83.372	214	suburban
130690002	Douglas	GA	Southeast	31.513	-82.750	64	rural
130890002	Panthersville	GA	Southeast	33.688	-84.290	244	suburban
131150005	Rome	GA	Southeast	34.263	-85.305	213	suburban
132150011	Columbus	GA	Southeast	32.431	-84.932	78	suburban
132450091	Augusta	GA	Southeast	33.434	-82.022	57	suburban
150032004	Pearl City	HI	Hawaii	21.397	-157.972	24	urban
170310057	Chicago	IL	Chicago	41.915	-87.723	185	suburban
170310076	Chicago	IL	Chicago	41.751	-87.714	188	suburban
170314201	Northbrook	IL	Chicago	42.140	-87.799	194	suburban
170434002	Naperville	IL	Chicago	41.771	-88.153	213	urban

Site	City	State	Region	Latitude (deg)	Longitude (deg)	Elevation (m)	Setting
171150013	Decatur	IL	Central U.S.	39.867	-88.926	206	suburban
171192009	Alton	IL	Central U.S.	38.903	-90.143	154	suburban
180372001	Jasper	IN	Ohio River Valley	38.391	-86.929	139	urban
180390003	Elkhart	IN	Michigan/Great Lakes	41.668	-85.969	229	urban
180650003	Middleton	IN	Ohio River Valley	40.012	-85.524	309	rural
180890022	Gary	IN	Michigan/Great Lakes	41.607	-87.305	179	urban
180892004	Hammond	IN	Michigan/Great Lakes	41.585	-87.474	182	urban
180970078	Indianapolis	IN	Ohio River Valley	39.811	-86.115	240	suburban
181630012	Evansville	IN	Ohio River Valley	38.022	-87.569	124	urban
191130037	Cedar Rapids	IA	Central U.S.	42.008	-91.679	254	urban
191530030	Des Moines	IA	Central U.S.	41.603	-93.643	282	urban
191630015	Davenport	IA	Central U.S.	41.530	-90.588	212	urban
201730010	Wichita	KS	Central U.S.	37.701	-97.314	405	urban
202090021	Kansas City	KS	Central U.S.	39.118	-94.636	269	urban
210190017	Ashland	KY	Ohio River Valley	38.459	-82.641	189	suburban
210670012	Lexington	KY	Ohio River Valley	38.065	-84.500	296	suburban
211110043	Louisville	KY	Ohio River Valley	38.233	-85.825	140	suburban
211170007	Covington	KY	Ohio River Valley	39.073	-84.525	220	suburban
211930003	Hazard	KY	Ohio River Valley	37.283	-83.220	414	suburban
220150008	Shreveport	LA	Mid South	32.534	-93.750	47	urban
220330009	Baton Rouge	LA	East Texas/Gulf	30.461	-91.177	16	urban
240053001	Essex	MD	Washington D.C. /Philadelphia Corridor	39.311	-76.474	10	suburban
240330030	Beltsville	MD	Washington D.C. /Philadelphia Corridor	39.055	-76.878	47	suburban
250130008	Westover AFB	MA	Northeast	42.195	-72.556	60	suburban
250250042	Boston	MA	Northeast	42.329	-71.083	5	urban
260770008	Kalamazoo	MI	Michigan/Great Lakes	42.278	-85.542	238	urban
260810020	Grand Rapids	MI	Michigan/Great Lakes	42.984	-85.671	190	urban
261130001	Houghton Lake	MI	Michigan/Great Lakes	44.311	-84.892	347	rural
261150005	Erie	MI	Michigan/Great Lakes	41.764	-83.472	175	rural
261610008	Ypsilanti	MI	Michigan/Great Lakes	42.241	-83.600	225	urban
261630001	Allen Park	MI	Michigan/Great Lakes	42.229	-83.208	182	suburban
261630033	Detroit	MI	Michigan/Great Lakes	42.307	-83.149	179	suburban
270530963	Minneapolis	MN	Central U.S.	44.955	-93.258	265	urban
271095008	Rochester	MN	Central U.S.	43.997	-92.450	318	suburban
280470008	Gulfport	MS	East Texas/Gulf	30.390	-89.050	6	rural
290470005	Liberty	MO	Central U.S.	39.303	-94.376	273	rural
290990012	Arnold	MO	Central U.S.	38.438	-90.361	150	suburban
291860005	Bonne Terre	MO	Central U.S.	37.897	-90.422	250	rural

Site	City	State	Region	Latitude (deg)	Longitude (deg)	Elevation (m)	Setting
295100085	St. Louis	MO	Central U.S.	38.656	-90.198	144	urban
300530018	Libby	MT	Northwest	48.384	-115.548	819	urban
300630031	Missoula	MT	Northwest	46.875	-113.995	1020	urban
310550019	Omaha	NE	Central U.S.	41.247	-95.976	347	suburban
320030020	Las Vegas	NV	Las Vegas	36.245	-115.092	583	urban
320030561	Las Vegas	NV	Las Vegas	36.164	-115.114	562	urban
320310016	Reno	NV	Northwest Nevada	39.525	-119.808	1403	urban
330150014	Portsmouth	NH	Northeast	43.075	-70.748	1	urban
340070003	Camden	NJ	Northeast	39.923	-75.098	2	suburban
340230006	New Brunswick	NJ	Northeast	40.473	-74.423	24	rural
340273001	Chester	NJ	Northeast	40.788	-74.676	256	rural
340390004	Elizabeth	NJ	Northeast	40.641	-74.208	3	suburban
350010023	Albuquerque	NM	Albuquerque	35.134	-106.586	1578	urban
360050110	Bronx	NY	New York City	40.816	-73.902	14	urban
360290005	Buffalo	NY	Northeast	42.877	-78.810	186	urban
360310003	Wilmington	NY	Northeast	44.393	-73.859	584	rural
360551007	Rochester	NY	Northeast	43.146	-77.548	146	urban
360610134	New York City	NY	New York City	40.714	-73.996	5	urban
360810124	Queens	NY	New York City	40.736	-73.823	13	suburban
361010003	Addison	NY	Northeast	42.091	-77.210	490	rural
370210034	Asheville	NC	Southeast	35.610	-82.351	706	suburban
370350004	Hickory	NC	Southeast	35.729	-81.366	341	suburban
370570002	Lexington	NC	Southeast	35.814	-80.263	237	urban
370670022	Winston-Salem	NC	Southeast	36.111	-80.227	279	urban
371070004	Kinston	NC	Southeast	35.232	-77.569	12	suburban
371190041	Charlotte	NC	Southeast	35.240	-80.786	223	urban
371590021	Rockwell	NC	Southeast	35.552	-80.395	224	rural
371830014	Raleigh	NC	Southeast	35.856	-78.574	92	suburban
380150003	Bismarck	ND	North Dakota	46.825	-100.768	548	suburban
380171004	Fargo	ND	North Dakota	46.934	-96.855	273	suburban
380530002	Watford City	ND	North Dakota	47.581	-103.300	629	rural
390171004	Middletown	OH	Ohio River Valley	39.530	-84.393	227	suburban
390350038	Cleveland	OH	Ohio River Valley	41.477	-81.682	186	urban
390350060	Cleveland	OH	Michigan/Great Lakes	41.494	-81.679	197	urban
390490081	Columbus	OH	Ohio River Valley	40.088	-82.960	263	suburban
390610040	Cincinatti	OH	Ohio River Valley	39.129	-84.504	213	urban
390870010	Ironton	OH	Ohio River Valley	38.520	-82.666	183	suburban
390933002	Sheffield	OH	Michigan/Great Lakes	41.463	-82.114	182	suburban
390950026	Toledo	OH	Michigan/Great Lakes	41.621	-83.641	191	suburban
390990014	Youngstown	OH	Ohio River Valley	41.096	-80.658	281	urban
391130031	Dayton	OH	Ohio River Valley	39.759	-84.144	250	suburban
391130032	Dayton	OH	Ohio River Valley	39.760	-84.188	242	urban
391510017	Canton	OH	Ohio River Valley	40.787	-81.394	334	urban
391530023	Akron	OH	Ohio River Valley	41.088	-81.542	313	urban
401091037	Edmond	OK	Mid South	35.614	-97.475	344	suburban
401431127	Tulsa	OK	Mid South	36.205	-95.977	193	urban
410290133	Medford	OR	Oregon	42.314	-122.879	433	urban
410390060	Eugene	OR	Oregon	44.026	-123.084	183	urban
410510080	Portland	OR	Oregon	45.497	-122.602	86	suburban

Site	City	State	Region	Latitude (deg)	Longitude (deg)	Elevation (m)	Setting
410510246	Portland	OR	Oregon	45.561	-122.679	61	urban
410610119	La Grande	OR	Northwest	45.339	-117.905	916	urban
420010001	Arendtsville	PA	Northeast	39.920	-77.310	241	rural
420030008	Pittsburgh	PA	Ohio River Valley	40.466	-79.961	312	suburban
420030064	Liberty	PA	Ohio River Valley	40.324	-79.868	279	suburban
420270100	State College	PA	Northeast	40.811	-77.877	354	rural
420290100	Toughkenamon	PA	Washington D.C. /Philadelphia Corridor	39.834	-75.769	91	rural
420430401	Harrisburg	PA	Northeast	40.245	-76.845	125	rural
420450002	Chester	PA	Washington D.C. /Philadelphia Corridor	39.836	-75.373	1	urban
420490003	Erie	PA	Northeast	42.142	-80.039	202	suburban
420692006	Scranton	PA	Northeast	41.443	-75.623	265	suburban
420710007	Lancaster	PA	Northeast	40.047	-76.283	99	suburban
420950025	Freemansburg	PA	Northeast	40.628	-75.341	93	suburban
421010004	Philadelphia	PA	Washington D.C. /Philadelphia Corridor	40.009	-75.098	25	urban
421010055	Philadelphia	PA	Washington D.C. /Philadelphia Corridor	39.923	-75.187	12	urban
421255001	Burgettstown	PA	Ohio River Valley	40.445	-80.421	344	rural
421290008	Greensburg	PA	Ohio River Valley	40.305	-79.506	378	suburban
421330008	York	PA	Northeast	39.965	-76.699	125	suburban
440070022	Providence	RI	Northeast	41.808	-71.415	17	urban
450190049	Charleston	SC	Southeast	32.791	-79.959	0	urban
450250001	Chesterfield	SC	Southeast	34.615	-80.199	122	rural
450450009	Taylors	SC	Southeast	34.901	-82.313	300	suburban
450790019	Columbia	SC	Southeast	33.993	-81.024	62	urban
460990006	Sioux Falls	SD	Central U.S.	43.544	-96.726	439	urban
470370023	Nashville	TN	Southeast	36.176	-86.739	153	urban
470654002	Chattanooga	TN	Southeast	35.051	-85.293	258	urban
470931020	Knoxville	TN	Southeast	36.019	-83.874	309	suburban
470990002	Loretto	TN	Southeast	35.116	-87.470	230	rural
471251009	Clarksville	TN	Southeast	36.514	-87.328	139	suburban
471570024	Memphis	TN	Southeast	35.151	-90.041	74	suburban
471631007	Kingsport	TN	Southeast	36.541	-82.522	394	suburban
481130069	Dallas	TX	Dallas	32.820	-96.860	132	urban
482011039	Deer Park	TX	East Texas/Gulf	29.670	-95.129	9	suburban
490110004	Bountiful	UT	Utah	40.903	-111.885	1307	suburban
490353006	Salt Lake City	UT	Utah	40.736	-111.872	1309	suburban
490494001	Lindon	UT	Utah	40.341	-111.714	1456	suburban
500070012	Burlington	VT	Northeast	44.480	-73.214	42	urban
510870014	Richmond	VA	Southeast	37.558	-77.400	34	suburban
530330080	Seattle	WA	Puget Sound	47.570	-122.309	58	urban
530530029	Tacoma	WA	Puget Sound	47.186	-122.452	97	suburban
530630016	Spokane	WA	Northwest	47.661	-117.357	596	suburban
540390011	Charleston	WV	Ohio River Valley	38.449	-81.684	264	rural
540391005	Charleston	WV	Ohio River Valley	38.368	-81.694	206	suburban
540511002	Moundsville	WV	Ohio River Valley	39.916	-80.734	245	suburban

Site	City	State	Region	Latitude (deg)	Longitude (deg)	Elevation (m)	Setting
550270007	Mayville	WI	Central U.S.	43.435	-88.528	348	rural
550790026	Milwaukee	WI	Central U.S.	43.061	-87.913	216	urban
551198001	Perkinstown	WI	Central U.S.	45.204	-90.600	449	rural
551330027	Waukesha	WI	Central U.S.	43.020	-88.215	263	urban

The IMPROVE and CSN networks operate collocated samplers in several urban/suburban sites. Collocated sites with data that met the completeness criteria outlined in Chapter 2 were compared to identify relative biases between IMPROVE and CSN speciated aerosol concentrations. We used daily data from Baltimore, Birmingham, Fresno, New York City, Phoenix, Puget Sound, and Washington, D.C., for 2005–2008. We compared ammonium sulfate (AS), ammonium nitrate (AN), organic carbon (OC), light absorbing carbon (LAC), soil, sea salt, $PM_{2.5}$ gravimetric fine mass (FM), and reconstructed fine mass (RCFM). Descriptions of how species mass was calculated are listed in Table 2.1 in Chapter 2.

Scatter plots of comparisons between IMPROVE and CSN species mass concentrations for all sites and years are presented in Figure 1.10. A summary of results is provided in Table 1.9. Errors were fairly low for most species (<20%), with the exception of soil (37.0%) and sea salt (78.3%), which also had high relative biases. IMPROVE sea salt concentrations were computed as 1.8 times chloride ion concentrations, whereas CSN sea salt concentrations were computed as 1.8 times chlorine concentrations. However, biases for other species were generally low, ranging from 5.7% for LAC to 18.4% for FM. The errors and relative biases between unadjusted CSN carbon and IMPROVE carbon data were 95.9% and 111.2 % for OC, respectively, and 26.7% and -17.3% for unadjusted LAC, respectively. The close agreement in OC and LAC suggests that the adjustments applied to those data were appropriate and effective (see Chapter 2). It should also be noted that while IMPROVE applies artifact corrections to ion data, CSN does not; some of the discrepancy between ion data from the two networks could be due to this difference.

It is worth discussing the relative biases associated with RCFM and FM. Relative biases in RCFM were low (0.04%) due to close agreement in the concentration of other major species, especially the adjusted CSN carbon concentrations. However, CSN FM concentrations were higher than IMPROVE FM concentrations on average, with a relative bias of 18.4%. As discussed in Chapter 2 and Chapter 8, OC concentrations measured by CSN samplers are roughly 20% higher than those obtained with IMPROVE samplers, most likely due to differences in filter face velocities and associated sampling artifacts between the two networks. The IMPROVE sampler has a much higher filter face velocity compared to the samplers used by CSN (Malm et al., 2011; Rattigan et al., 2011). Negative artifacts associated with the sampling systems also likely affect FM measurements on Teflon filters, and contribute to the relative bias in FM concentrations between the two networks. In this report, CSN carbon data have been adjusted for sampling artifacts to agree with IMPROVE carbon data, but FM data have not. Comparisons of FM and RCFM for CSN data are affected by this discrepancy, which may be an issue now that CSN has completed the transition to the URG 3000N sampling system for its carbon monitoring, but maintains its FM measurement using samplers with much lower filter face velocities. Examples of the effects of this discrepancy are presented in Chapter 2.2.9 with the comparison of FM and RCFM for the CSN and IMPROVE network.

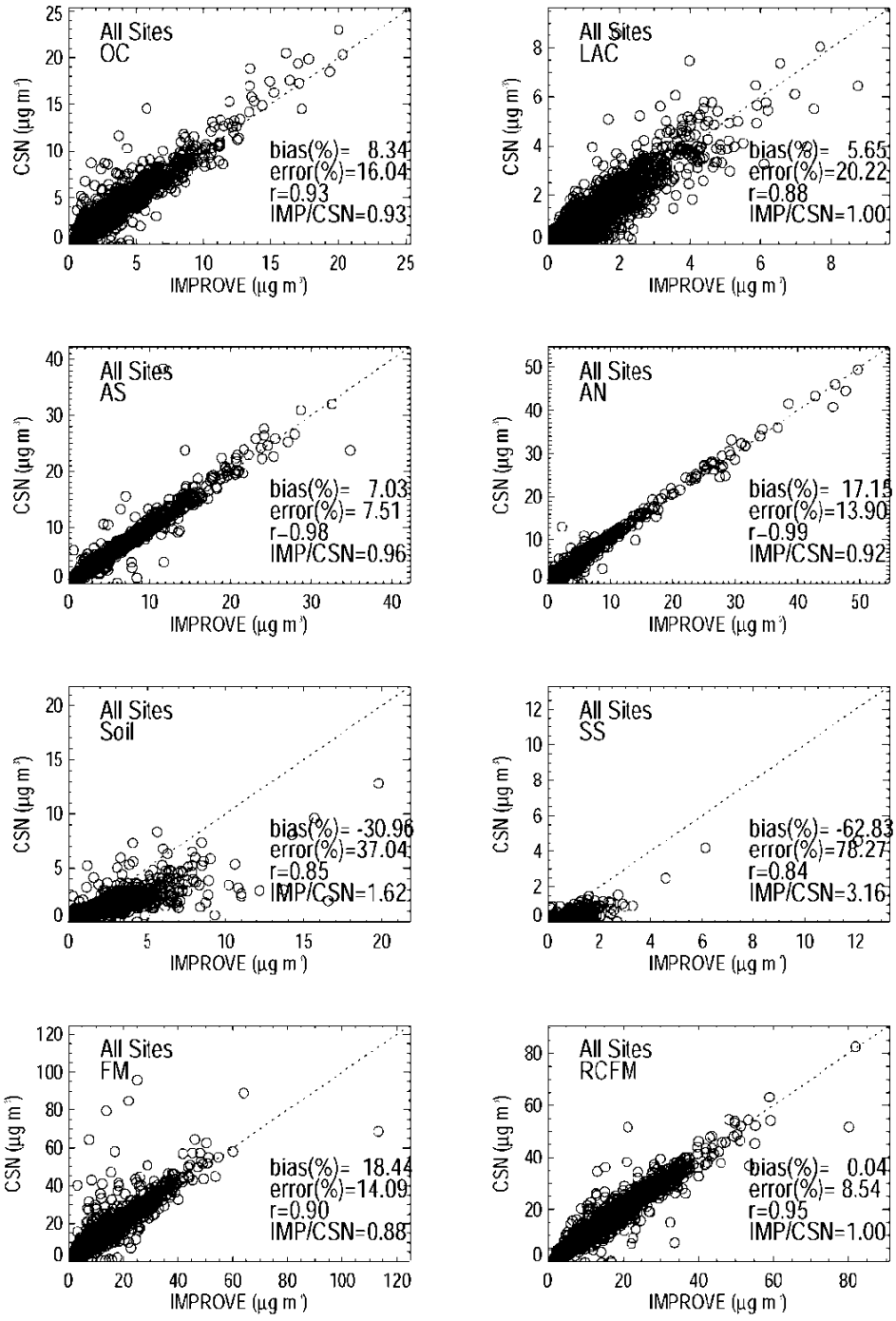

Figure 1.10. Comparisons of 2005–2008 aerosol mass concentration data (µg m^{-3}) for seven collocated IMPROVE and CSN sites (see text) for adjusted organic carbon (OC), adjusted light absorbing carbon (LAC), ammonium sulfate (AS), ammonium nitrate (AN), soil, sea salt (SS), $PM_{2.5}$ gravimetric fine mass (FM), and $PM_{2.5}$ reconstructed fine mass (RCFM).

The large errors and relative biases for soil and sea salt indicate that IMPROVE had much higher soil and sea salt mass concentrations compared to CSN. Recall that these data are from collocated sites, so the relative biases stem from differences in sampling or analytical techniques. As discussed in Chapter 2, sea salt is computed as 1.8 times chloride ion concentrations for IMPROVE and 1.8 times chlorine concentrations from the CSN (the CSN does not report chloride ion concentrations). Relative biases in sea salt reflect differences in these measurements and analyses. The relative biases in soil and sea salt mass concentrations are sufficiently large that combined data analyses should be treated as semiquantitative. CSN concentrations were somewhat higher than IMPROVE concentrations for most species (positive relative biases correspond to higher CSN concentrations), but data from the two networks were fairly highly correlated. The general agreement for most species indicates that the data can be combined.

Comparisons between IMPROVE and CSN data are separated by site and year and presented in Appendix A. Similar comparisons of elemental species used to construct soil and sea salt mass concentrations (Al, Si, Ca, Fe, Ti, and Cl^-, see Chapter 2) are also presented in Appendix A, as are comparisons between unadjusted and adjusted carbon data.

Table 1.9. Comparisons between collocated IMPROVE and CSN sites for all data from 2005 through 2008. Species include organic carbon (OC), light absorbing carbon (LAC), ammonium sulfate (AS), ammonium nitrate (AN), soil, sea salt, $PM_{2.5}$ gravimetric fine mass (FM), and $PM_{2.5}$ reconstructed fine mass (RCFM). "OC_{unadj}" and "LAC_{unadj}" refer to comparisons between unadjusted CSN carbon data and IMPROVE carbon data; "OC_{adj}" and "LAC_{adj}" refer tocomparisons between adjusted CSN carbon and IMPROVE carbon data.

Statistic	OC_{unadj}	LAC_{unadj}	OC_{adj}	LAC_{adj}	AS[3]	AN[4]	Soil	Sea salt[5]	FM	RCFM
Average IMPROVE ($\mu g\ m^{-3}$)	2.8	1.3	2.7	1.2	3.9	2.3	1.4	0.3	12.6	13.5
Average CSN ($\mu g\ m^{-3}$)	5.2	1.0	3.0	1.2	4.1	2.6	0.9	0.11	14.3	13.5
Bias[1] (%)	111.2	-17.3	8.3	5.7	7.0	17.2	-31.0	-62.8	18.4	0.04
Error[2] (%)	95.9	26.7	16.0	20.2	7.5	13.9	37.0	78.3	14.1	8.5
r	0.92	0.87	0.93	0.88	0.98	0.99	0.85	0.84	0.9	0.95
IMP/CSN	0.54	1.3	0.93	1.0	0.96	0.92	1.6	3.2	0.9	1.0
Number of data points (N)	2087	2077	2675	2665	2687	2689	2646	1904	2636	2535

[1] $\text{Error} = \text{median}\left(\left|\frac{\overline{X}_i - \overline{Y}_i}{\overline{Y}_i}\right|\right)$

[2] $\text{Bias} = \frac{1}{N}\sum_i^N \frac{\overline{X}_i - \overline{Y}_i}{\overline{Y}_i}$; $\overline{X}_i$ and $\overline{Y}_i$ are the daily data for CSN and IMPROVE concentrations, respectively. The number of data points is given by N.

[3] AS = 1.375[sulfate ion]

[4] AN = 1.29[nitrate ion]

[5] Sea salt = 1.8[chloride ion] for IMPROVE and 1.8[chlorine] for CSN.

REFERENCES

Bond, T. C., and R. W. Bergstrom (2006), Light absorption by carbonaceous particles: An investigative review, *Aerosol Sci. Techno., 40,* 27-67.

Chow, J. C., J. G Watson, L. C. Pritchett, W. R. Pierson, C A. Frazier, and R G. Purcell (1993), The DRI thermal/optical reflectance carbon analysis system: description, evaluation, and applications in U.S. air quality studies, *Atmos. Environ*., *27(A)*(8), 1185-1201.

Chow, J. C., J. G. Watson, L.-W. Antony Chen, M.-C. Oliver Chang, G. Paredes-Miranda (2005), Comparison of the DRI/OGC and Model 2001 Thermal/Optical Carbon Analyzers, http://vista.cira.colostate.edu/improve/Publications/GrayLit/013_CarbonAnalyzer/IMPROVECarbonAnalyzerAssessment.pdf.

Chow, J. C., J. G. Watson, L.-W.A. Chen, J. Rice, and N. H. Frank (2010), Quantification of $PM_{2.5}$ organic carbon sampling artifacts in U.S. networks, *Atmos. Chem. Phys., 10,* 5223-5339.

Debell, L. J., K. Gebhart, J. L. Hand, W. C. Malm, M. L. Pitchford, B. A. Schichtel, and W. H. White (2006), IMPROVE (Interagency Monitoring of Protected Visual Environments): Spatial and seasonal patterns and temporal variability of haze and its constituents in the United States: Report IV, CIRA Report ISSN: 0737-5352-74, Colo. State Univ., Fort Collins.

Dietrich, D.L., J. D. Molenar, and J. F. Faust (1989), Transmissometer extinction measurements in an urban environment, In *Visibility and Fine Particles*, C.V. Mathai, Ed., AWMA, Pittsburgh, pages 374-383.

Dillner, A. M., C. H. Phuah, and J. R. Turner (2009), Effects of post-sampling conditions on ambient carbon aerosol filter measurements, *Atmos. Environ., 43,* 5937-5943.

Flocchini, R. (2007), Shifts in Mo-anode XRF element calibration factors, Doc. # da0014, http://vista.cira.colostate.edu/improve/Data/QA_QC/Advisory/da0014/da0014_Mo_drop.pdf.

Hand, J. L., W. C. Malm, A. Laskin, D. Day, T. Lee, C. Wang, C. Carrico, J. Carrillo, J. P. Cowin, J. Collett, Jr., and M. J. Iedema (2005), Optical, physical, and chemical properties of tar balls observed during the Yosemite Aerosol Characterization Study, *J. Geophys. Res., 110,* D21210, doi:10.1029/2004JD005728.

John, W., and G. Reischl (1980), A cyclone for size-selective sampling of air, *J. Air Poll. Contr. Assoc., 30,* 872-876.

Joseph, D. B., J. Metsa, W. C. Malm, and M. L. Pitchford (1987), Plans for IMPROVE: a federal program to monitor visibility in class I areas, In: *Visibility Protection: Research and Policy Aspects,* P.S. Bhardwaja (Ed.), APCA, Pittsburgh PA.

Malm, W. C., J. F. Sisler, D. Huffman, R. A. Eldred, and T. A. Cahill (1994), Spatial and seasonal trends in particle concentration and optical extinction in the United States, *J. Geo. Res*., *99*(D1), 1347-1370.

Malm, W. C., J. F. Sisler, M. L. Pitchford, M. Scruggs, R. Ames, S. Copeland, K. A. Gebhart, and D. E. Day (2000), IMPROVE (Interagency Monitoring of Protected Visual Environments): Spatial and seasonal patterns and temporal variability of haze and its constituents in the United States: Report III, CIRA Report ISSN: 0737-5352-47, Colo. State Univ., Fort Collins, http://vista.cira.colostate.edu/improve/Publications/Reports/2000/2000.htm.

McDade, C. E., R. A. Eldred, and L. L. Ashbaugh (2004), Artifact corrections in IMPROVE, internal report.

McDade, C. E. (2007), Change in definition of flowrate native flags, Doc. # da0015, http://vista.cira.colostate.edu/improve/Data/QA_QC/Advisory/da0015/da0015_NewFlowFlags.pdf.

Molenar, J. F, D. L. Dietrich, and R. M. Tree (1989), Application of a long-range transmissometer to measure the ambient atmospheric extinction coefficient in remote pristine environments, In *Visibility and Fine Particles*, C.V. Mathai, Ed., AWMA, Pittsburgh, 374-383.

Molenar, J. F., and W. C. Malm (1992), Ambient optical monitoring techniques, presented at the Conference on Visibility and Fine Particles, Vienna, Austria, September.

Pitchford, M. L., and W. C. Malm (1994), Development and applications of a standard visual index, *Atmos. Environ., 28(*5*),* 1049-1054.

Rattigan, O. V., H. D. Felton, M.-S. Bae, J. J. Schwab, K. L. Demerjian (2011), Comparison of long-term $PM_{2.5}$ carbon measurements at an urban and rural location in New York, *Atmos. Environ., 45,* 3228-3236.

Sisler, J. F. (1996), Spatial and seasonal patterns and long term variability of the composition of the haze in the United States: An analysis of data from the IMPROVE network, Cooperative Institute for Research in the Atmosphere, Colorado State University, ISSN 0737-5352-32.

Turner, J. R. (2006), personal communication.

U.S. EPA (1999a), Regional Haze Regulations; Final Rule, 40 CFR 51, Federal Register, 64, 35714-35774.

U.S. EPA (1999b), Visibility Monitoring Guidance, Office of Air Quality Planning and Standards, Research Triangle Park, NC 27711, EPA-454/R-99-003.

U.S. EPA (2004), PM2.5 Speciation Network Newsletter, Volume 1, Issue 1, (http://www.epa.gov/ttn/amtic/files/ambient/pm25/spec/spnews1.pdf)

U.S. EPA (2009), PM2.5 Speciation Network Newsletter, Issue 6, Summer 2009, (http://www.epa.gov/ttn/amtic/files/ambient/pm25/spec/spnews6.pdf).

Watson, J. G., J. C. Chow, L.-W.A. Chen, N. H. Frank (2009), Methods to assess carbonaceous aerosol sampling artifacts for IMPROVE and other long-term networks, *J. Air Waste Manage. Assoc., 59,* 898-911.

White, W. (2006a), Changed reporting of XRF sulfur, Doc. # da0009, http://vista.cira.colostate.edu/improve/Data/QA_QC/Advisory/da0009/da0009_S_reporting.pdf.

White, W. (2006b), S interference in XRF determination of Si, Doc. # da0011, http://vista.cira.colostate.edu/improve/Data/QA_QC/Advisory/da0011/da0011_S_Si.pdf.

White, W. (2007a), Shift in EC/OC split with 1 January 2005 TOR harware upgrade, Doc. # da0016, http://vista.cira.colostate.edu/improve/Data/QA_QC/Advisory/da0016/da0016_TOR2005.pdf.

White, W. (2007b), Changes in sodium data quality, Doc. # da0017, http://vista.cira.colostate.edu/improve/Data/QA_QC/Advisory/da0017/da0017_Na.pdf.

White, W. (2007c), Introduction of a second copper-anode XRF system, Doc. # da0013, http://vista.cira.colostate.edu/improve/Data/QA_QC/Advisory/da0013/da0013_TwoVacs.pdf.

White, W. (2007d), Varying bias in XRF sulfur relative to IC sulfate, Doc. # da0012, http://vista.cira.colostate.edu/improve/Data/QA_QC/Advisory/da0012/da0012_SSO4.pdf.

White, W. (2008), Bias between masked and unmasked elemental measurements, Doc. # da0019, http://vista.cira.colostate.edu/improve/Data/QA_QC/Advisory/da0019/da0019_masks.pdf.

White, W. (2009), Inconstant bias in XRF sulfur- Advisory Update to da0012, Doc. # da0023, http://vista.cira.colostate.edu/improve/Data/QA_QC/Advisory/da0023/da0023_DA_SSO4_update.pdf.

White, W. (2010), Bias between masked and unmasked light absorption measurements, Doc. # da0028, http://vista.cira.colostate.edu/improve/Data/QA_QC/Advisory/da0028/da0028_DA_mask_Fabs.pdf.

Yu, X-Y., T. Lee, B. Ayres, S. M. Kreidenweis, J. L. Collett, Jr., and W. C. Malm (2005), Particulate nitrate measurement using nylon filters, *J. Air Waste Manage. Assoc., 55,* 1100-1110.